



Review

# Remote Sensing Data for Digital Soil Mapping in French Research—A Review

Anne C. Richer-de-Forges <sup>1</sup>, Qianqian Chen <sup>1,2</sup>, Nicolas Baghdadi <sup>3</sup>, Songchao Chen <sup>4,5</sup>, Cécile Gomez <sup>6</sup>, Stéphane Jacquemoud <sup>7</sup>, Guillaume Martelet <sup>8</sup>, Vera L. Mulder <sup>9</sup>, Diego Urbina-Salazar <sup>2</sup>, Emmanuelle Vaudour <sup>2</sup>, Marie Weiss <sup>10</sup>, Jean-Pierre Wigneron <sup>11</sup> and Dominique Arrouays <sup>1,\*</sup>

<sup>1</sup> INRAE, Info&Sols, 45075 Orléans, France; anne.richer-de-forges@inrae.fr (A.C.R.-d.-F.); qianqian.chen@inrae.fr (Q.C.)

<sup>2</sup> University Paris-Saclay, INRAE, AgroParisTech, UMR EcoSys, 91120 Palaiseau, France; diego.urbina-salazar@inrae.fr (D.U.-S.); emmanuelle.vaudour@inrae.fr (E.V.)

<sup>3</sup> TETIS, University Montpellier, INRAE, CIRAD, AgroparisTech, 91120 Palaiseau, France; nicolas.baghdadi@teledetection.fr

<sup>4</sup> ZJU-Hangzhou Global Scientific and Technological Innovation Center, Zhejiang University, Hangzhou 311215, China; chensongchao@zju.edu.cn

<sup>5</sup> College of Environmental and Resource Sciences, Zhejiang University, Hangzhou 310058, China

<sup>6</sup> LISAH, University Montpellier, IRD, INRAE, Institut Agro Montpellier, 34060 Occitanie Montpellier, France; cecile.gomez@ird.fr

<sup>7</sup> CNRS, Institut de Physique du Globe de Paris, University Paris Cité, 75005 Paris, France; jacquemoud@ipggp.fr

<sup>8</sup> BRGM, UMR 7327, 45060 Orléans, France; g.martelet@brgm.fr

<sup>9</sup> Soil Geography and Landscape Group, Wageningen University, P.O. Box 47, 6700 AA Wageningen, The Netherlands; titia.mulder@wur.nl

<sup>10</sup> INRAE, Avignon Université, EMMAH, 84000 Avignon, France; marie.weiss@inrae.fr

<sup>11</sup> INRAE ISPA, Centre de Bordeaux-Aquitaine, 33140 Villenave d'Ornon, France; jean-pierre.wigneron@inrae.fr

\* Correspondence: dominique.arrouays@inrae.fr

**Abstract:** Soils are at the crossroads of many existential issues that humanity is currently facing. Soils are a finite resource that is under threat, mainly due to human pressure. There is an urgent need to map and monitor them at field, regional, and global scales in order to improve their management and prevent their degradation. This remains a challenge due to the high and often complex spatial variability inherent to soils. Over the last four decades, major research efforts in the field of pedometrics have led to the development of methods allowing to capture the complex nature of soils. As a result, digital soil mapping (DSM) approaches have been developed for quantifying soils in space and time. DSM and monitoring have become operational thanks to the harmonization of soil databases, advances in spatial modeling and machine learning, and the increasing availability of spatiotemporal covariates, including the exponential increase in freely available remote sensing (RS) data. The latter boosted research in DSM, allowing the mapping of soils at high resolution and assessing the changes through time. We present a review of the main contributions and developments of French (inter)national research, which has a long history in both RS and DSM. Thanks to the French SPOT satellite constellation that started in the early 1980s, the French RS and soil research communities have pioneered DSM using remote sensing. This review describes the data, tools, and methods using RS imagery to support the spatial predictions of a wide range of soil properties and discusses their pros and cons. The review demonstrates that RS data are frequently used in soil mapping (i) by considering them as a substitute for analytical measurements, or (ii) by considering them as covariates related to the controlling factors of soil formation and evolution. It further highlights the great potential of RS imagery to improve DSM, and provides an overview of the main challenges and prospects related to digital soil mapping and future sensors. This opens up broad prospects for the use of RS for DSM and natural resource monitoring.

**Keywords:** remote sensing; soil digital soil mapping; scale; sampling density; resolution; sensors; wavelengths; covariates; review



**Citation:** Richer-de-Forges, A.C.; Chen, Q.; Baghdadi, N.; Chen, S.; Gomez, C.; Jacquemoud, S.; Martelet, G.; Mulder, V.L.; Urbina-Salazar, D.; Vaudour, E.; et al. Remote Sensing Data for Digital Soil Mapping in French Research—A Review. *Remote Sens.* **2023**, *15*, 3070. <https://doi.org/10.3390/rs15123070>

Academic Editor: Peng Fu

Received: 28 April 2023

Revised: 1 June 2023

Accepted: 9 June 2023

Published: 12 June 2023



**Copyright:** © 2023 by the authors. Licensee MDPI, Basel, Switzerland. This article is an open access article distributed under the terms and conditions of the Creative Commons Attribution (CC BY) license (<https://creativecommons.org/licenses/by/4.0/>).

## 1. Introduction

Soils are a key component of the Critical Zone and a limited resource. They are essential to addressing the climate crisis we are facing. Soils are at the crossroads of existential issues such as food and water security and safety, climate change mitigation, and adaptation, human health, sustainable energy, and biodiversity protection [1,2]. Yet, around the world, they are under threat [3,4], even though they are essential for achieving most of the sustainable development goals (e.g., [5–8]). These threats continue to grow under human pressure [3,4]. To address this problem, policy initiatives are emerging in Europe, such as the Soil Thematic Strategy [9] or the E.U. Mission “A Soil Deal for Europe” [10]. There is an urgent need to map and monitor soils at field, regional, and global scales in order to improve their management and prevent their degradation. This remains a challenge due to the high/complex spatial variability inherent in soils. Providing such information by mapping and monitoring soil properties in a reproducible way is now possible through Digital Soil Mapping (DSM, [11]). The concept of DSM has rapidly developed and become operational thanks to the harmonization of soil databases, advances in spatial modeling and machine learning, and the increasing availability of spatial covariates [12,13], including the considerable increase in remote sensing data.

DSM emerged in the early 2000s [11,14] as a new concept for mapping soil properties and/or soil classes using soil information and spatially comprehensive covariates, which builds on the work of Jenny [15]. In their seminal article, McBratney et al. [11] proposed a framework called the scorpan-SSPF<sub>e</sub>. This framework included a soil spatial prediction function for soil mapping with spatially auto-correlated errors, often referred to as SCORPAN. As defined by McBratney et al. [11], SCORPAN is based on seven predictive factors of soil types or soil attributes, namely: (1) *s*: soil, other or previously measured attributes of the soil at a point; (2) *c*: climate, climatic properties of the environment at a point; (3) *o*: organisms, including land cover and natural vegetation; (4) *r*: topography, including terrain attributes and classes; (5) *p*: parent material, including lithology; (6) *a*: age, the time factor; (7) *n*: space, spatial or geographic position.

The prediction functions can use a wide variety of statistical tools, including regression, classification, geostatistics, machine learning, etc. It is not the purpose of this review to detail these methods or their advantages and limitations. We refer to McBratney et al. [11], Grunwald [16], Minasny and McBratney [12,17], Zhang et al. [18], Wadoux et al. [19], Arrouays et al. [20], Wadoux et al. [19] and Chen et al. [21].

A recent trend is that the availability of RS products, and in particular those derived from satellite [22], airborne, or unmanned aerial vehicle (UAV) imagery [23], has increased significantly. Thus, almost all DSM approaches rely on RS data to obtain spatially exhaustive environmental covariates [21], as well as legacy soil, geology, geomorphology, and landforms maps. Ustin and Middleton [24] identified and described 48 instruments and 13 multi-instrument platforms that collected data in the 2000s, were recently launched, or are expected to be launched in this decade. Indeed, some of these are now being considered as a direct measurement of some targeted soil properties [25]. Commercial operations are also entering the market, providing competitive products with high spatiotemporal (e.g., Planet, <https://www.planet.com/products/planet-imagery/> accessed on 29 May 2023 or EarthDaily <https://earthdaily.com/earthdaily/> accessed on 29 May 2023) and even spectral resolution (e.g., Kuva Space, <https://kuvaspace.com/> accessed on 29 May 2023). In this review, we mainly focus on satellite and airborne imagery as we aim to review DSM studies covering rather large areas. Nevertheless, we do not totally exclude examples on UAV when they are relevant for field- or farm-scale soil mapping or monitoring.

French research has a long history in the field of soil RS. As early as the early 1960s, they developed innovative approaches for the photo-interpretation of aerial photographs for soil mapping [26–28], visual interpretation, and/or digital processing of RS images. It was stimulated by the launch of the first Earth observation satellite, Landsat, in 1972 and, in 1986, the French *Satellite Probatoire d’Observation de la Terre* (SPOT). Some pioneering French works include general books on RS applications to the characterization of the biosphere or

terrestrial environment (e.g., [29–34]). The development of soil RS was notably based on French research focused on the spectral characterization of minerals [35–37] and on the soil surface status [38–48]. In the latter case, the aim was to define soil spectral indices such as the widely used brightness index [49–51], the Transformed Soil-Adjusted Vegetation Index (TSAVI) [52], and the theorization of the soil line concept [53]. This led to the physical modeling of soil bidirectional reflectance [54,55] thanks to the SOILSPECT model of S. Jacquemoud [56], which was followed by the MARMIT model of A. Bablet [57,58]. The same thing has happened in the microwave and thermal infrared domains [59,60].

Observation and hence, understanding the spectral behavior of soil as a function of its composition and structure has been the cornerstone for establishing relationships between the spatial distribution of soil properties at different scales, soil types, or soilscapes, and RS imagery products in the solar (e.g., [61–77]), as well as in the microwave (e.g., [65,70,71,73]) and the thermal infrared (e.g., [59,78,79]) domains. Several studies have also addressed the mapping of soil color (e.g., [46,51,80]) or soil moisture (e.g., [78,79,81–86]). Others aimed to consider the bare soil surface reflectance, roughness, rockiness, or soil cover by vegetation or crop residues for several applications: modeling/mapping of soil crusting, surface water runoff, erodibility or erosion risk (e.g., [40,47,87–98]), and salinity [41,48,99–101].

Vegetation is a problem for direct RS of some primary soil properties that are easier to capture by images acquired on bare soils [102]. Therefore, several works have attempted to develop vegetation indexes that are nearly insensitive to the soil spectral response, unlike the NDVI (e.g., [103,104]). However, (i) vegetation is one of the main controlling factors of soil evolution (e.g., inputs in soil organic carbon and influence on pH); (ii) vegetation information may also be related to some soil properties that are not easily detected using only soil surface response (e.g., soil depth and available water capacity (AWC)) and thus need to be captured for DSM.

Comprehensive reviews of the use of remote sensing for soil and terrain mapping were made from the French research as early as 1974, albeit in French [31,105], and major reviews were later published in English by Ben-Dor et al. [106,107], Ben-Dor [108], and Mulder et al. [109]. The latter introduced the use of RS as primary or secondary soil data to improve DSM. As RS products have become increasingly available and diverse and also offer higher resolutions in space, time, and spectral range, updated reviews have been published by Dematté et al. [110] and Chabrillat et al. [111], focusing on the main soil characteristics monitored by RS and the perspectives offered by new sensors [112].

The idea of an article gathering the specific contributions of RS to DSM from French research originates from a scientific working group founded in 2015 and named Theia “CNS for *Cartographie Numérique des Sols*” (DSM for Digital Soil Mapping). This French working group aims to federate the efforts of French research laboratories developing digital mapping approaches for perennial soil properties [113,114] under the supervision of *Centre National d’Etudes Spatiales* (French Space Agency). We believe that such an approach can be useful not only on a national scale, but that it can also be considered as the first step to implement a similar approach on a global scale.

The objectives of this review are as follows:

1. Summarize the main soil properties and threats that have been studied on a large scale over the last decade using RS by the French research community;
2. Synthesize the main recent methodological advances of DSM related to the use of RS products in France or elsewhere from French research;
3. Highlight the complementarity of the new RS products and the other covariates currently used in DSM.

## 2. General Considerations on the Relative Permanence of Soil Properties

DSM predicts soil properties that may change over different times, from brief sudden events to millions of years. Time intervals vary with soil properties and processes and are highly dependent on the controlling factors for soil formation and anthropogenic influences. These factors can be rather slow, such as weathering and pedogenesis, or

short-lived when related to destructive events, such as deforestation, erosion and flooding, or local contamination. RS technology has evolved rapidly over the last 50 years or so, providing greater diversity in spectral domains, but also a drastic increase in their spatial resolution and revisit time. This improves our understanding of the relative permanence of soil properties, yet it is limited to one week to half a century. In this section, we will refer mainly to the international literature, as many concepts have emerged outside the strict French soil science community.

Soils are continually evolving over time, and the rate of change in soil properties is accelerating due to global changes and continued unsustainable land management [2,4]. The “natural” formation time of soils, from the initial weathering of parent materials to pedogenic evolution, may range from about 10,000 to 2,500,000 years. As a result, the evolution and properties of natural soils mainly depend on age (time), climate (including past climates), parent material, and natural vegetation. It is generally accepted that the “age” factor is least used in DSM, except for some long periods of extreme climate (e.g., glaciation and interglacial periods) [16]. Therefore, the influence of past climate may be underestimated by DSM covariates and is often barely captured by RS products, as they do not cover the duration of most pedogenetic processes. Many soil properties have been affected by drastic changes since the impact of humans, especially by gradual or abrupt land-use changes. This began when humans moved from hunting and gathering to agriculture (Neolithic revolution). This then led to (ongoing) deforestation and the conversion of land to arable land, and more recently to global changes, such as anthropogenic climate change, industrialization, urbanization and increases in impervious surfaces, land-take, and changes in land use/land cover due to food demand. To differentiate the effects of long- and short-term periods on soil variability, researchers have proposed a distinction between genosoils and phenosoils [115]. This concept makes it possible to distinguish certain semi-permanent properties inherited from “natural” pedogenesis from properties that have evolved under human pressure, especially for the history of land use. It has led to further development and discussions of which soil properties can be considered more or less “permanent”, e.g., certain characteristics of deep diagnostic horizons [116], while others may change with land use, management (e.g., [117–120]), or under other circumstances. This concept is quite similar to the concept of soil capability vs. soil condition, as defined by McBratney et al. [1].

In this study, we will therefore make the assumption that certain soil attributes can be considered permanent (e.g., soil texture, soil mineralogy, and parent material) on the time-scale of RS observations (i.e., 50 years). Unless there is evidence that abrupt or destructive events have occurred, such as severe erosion or salinization. The typical duration of the semi-permanent changes can range from decades to centuries (e.g., soil organic carbon stocks and diffuse contaminant contents) to seasonal ones (e.g., deep horizon structure and permeability, pH, rooting depth, and soil temperature). Much more rapid and/or even nearly instantaneous changes are related to human actions or climate events, e.g., local contamination, nutrients content, topsoil structure and roughness, pH in limed cultivated soils, and, of course, soil moisture.

It is therefore important to keep these different times in mind, especially when dealing with soil data and/or RS acquisition dates, or the time-scales relevant to monitoring. Note that some information gathered by RS, and even by other DSM covariates (i.e., relief) might not reflect the variation of SCORPAN covariates over large time-scales.

### **3. Developments Related to the Extraction of Soil Properties from Remote Sensing Data**

#### *3.1. Use of RS Data as a Substitute for Soil Properties’ Measurement*

In many cases, RS data are directly used as a measure of soil properties, which Mulder et al. [109] called the “primary soil data source”. Bare soil reflectance, for example, has been correlated with many topsoil properties measured in the lab. A model or a spectral index is built to predict certain properties, a given behavior, or a threat to the soil from its spectral

reflectance at one or more wavelengths. Thus, many attempts have been made to determine soil moisture [121], soil carbon [122], soil clay content [123,124], or soil salinity [125].

In many cases, therefore, RS is not incorporated into a full SCORPAN model, but directly used as a predictor of the soil property of interest through generalized linear models, partial least squares regression (PLSR), geostatistics, machine learning, or other prediction tools (e.g., [126–129]). In this case, uncertainties and biases in the predictions should be noted, and care should be taken not to apply them outside their domain of validity. If the results are satisfactory, i.e., if RS data capture most of the variability of the soil attribute in a given area, it may not be necessary to incorporate them into a SCORPAN model (e.g., [123,124,130–132]).

Note that these considerations do not claim that working on the field and taking samples are not essential. Working on the field is a crucial step in DSM and RS for several reasons:

- Lab measurements performed on samples taken into the field are essential to calibrate RS and DSM predictions, and they must be representative from both feature and spatial domains (e.g., [12,106–112,126,127,133–135]).
- Using more high-resolution spatial covariates does not necessarily improve the prediction accuracy (e.g., [12,19,20,136]).
- Validation should involve appropriate sampling in the field (e.g., [12,17–21,123,126,127,131,132,137]).
- The lack of field data is often one of the main limiting factors of RS and DSM prediction performances (e.g., [13,21,138–143]).
- Soil knowledge acquired in the field is useful to improve and assess the RS and DSM prediction performances (e.g., [17,19–21,127,138,139,144–148]).

### 3.2. Most Studied Soil Properties in French Remote Sensing Research

In order to have an overview of the most studied soil properties in French RS research, a dedicated bibliographic search was performed using the Clarivate Web of Science. The query returned 2426 articles, which shows a high productivity. Figure 1 shows the relative percentage of the main soil properties selected, and we decided to focus on those properties that exceed 5% of the total number of French research papers. We recognize that there is no guarantee that the search is exhaustive, given the query process. However, to our knowledge, this is the best effort of such a systematic literature search related to French soil RS research.

The most studied soil property is soil moisture (usually topsoil moisture), which has been studied either in the solar domain (e.g., [39,57–59,78]), the thermal infrared domain [59,60,78,79], or the microwave domain (e.g., [84,86,149–159]).

Soil moisture is one of the most studied soil properties in France and can be mainly related to the ESA SMOS (Soil Moisture and Ocean Salinity) mission. The origin of SMOS goes back to the early 1990s. As part of the development of passive microwave radiometers by CNES, experiments were conducted over crop fields in 1991 and 1993 in the remote sensing facilities of INRAE in Avignon. Wigneron et al. [160,161] demonstrated the possibility to simultaneously extract soil moisture (SM) and Vegetation Optical Depth (VOD), a parameter related to the vegetation water content, from multi-angular and bi-polarization passive microwave (MW) observations. Shortly after, Wigneron et al. [133,162] defined a retrieval algorithm based on the inversion of the L-MEB model (L-band Microwave Emission of the Biosphere). This algorithm, which is well suited for a spaceborne mission, was the core of a research proposal submitted to the ESA Call for Earth Explorer Missions. The proposal was accepted by ESA in 1999 (phase A), leading to the Soil Moisture and Ocean Salinity (SMOS) mission coordinated by Y. Kerr, its principal investigator [163]. The satellite was launched at the end of 2009 as part of the ESA Living Planet Programme. In parallel, many scientific advances have been made in the domain of active microwaves (radar) with the support of CNES. It is more difficult to extract SM from active MV sensors (i.e., scatterometers and Synthetic Aperture Radar (SAR)) than from passive sensors (i.e., radiometers). In active RS,

measurements must take into account complex extinction effects due to vegetation structure and complex scattering effects due to soil roughness. However, while the spatial resolution of passive MW radiometers is limited to 35–50 km, that of active SAR systems can reach a few meters. Thus, the SM products retrieved from passive MW with low spatial resolutions mainly have applications in hydrology, climate studies, and meteorology [153], while the SM products retrieved from active systems can also find applications in agriculture [164].

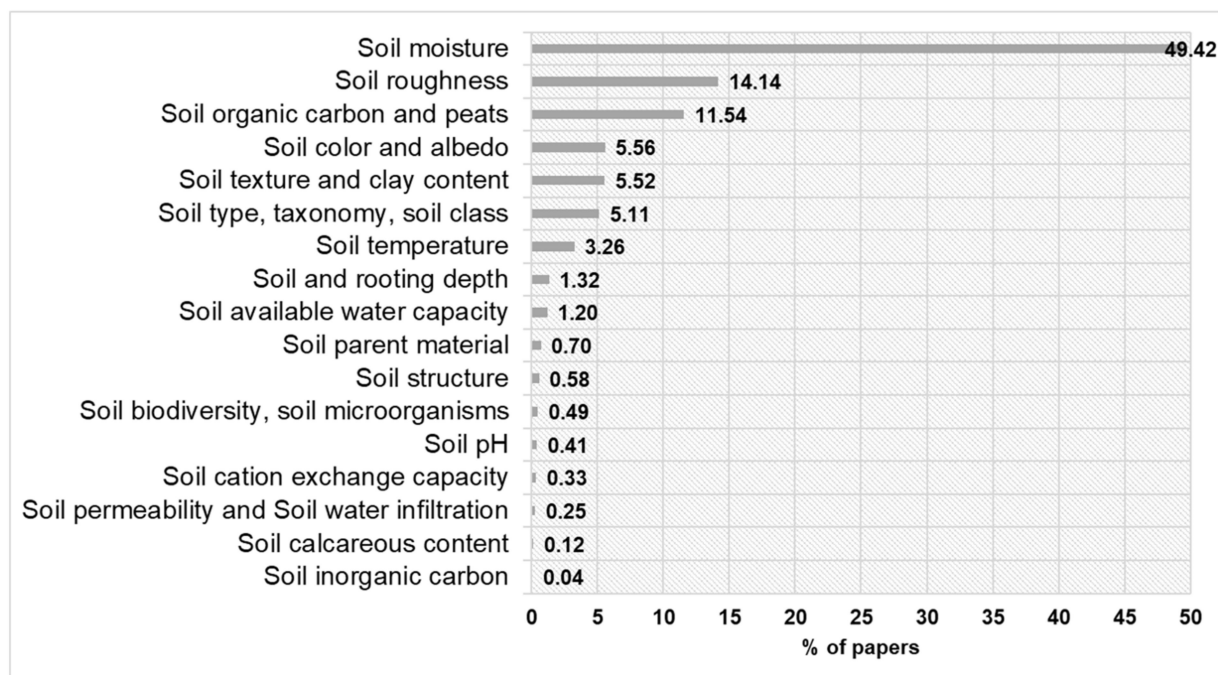


**Figure 1.** Percentage of articles by soil properties published by French researchers (out of 2426 articles). This citation report graphic is derived from Clarivate Web of Science, Copyright Clarivate 2022. All rights reserved. We selected articles whose TITLE, TOPIC, KEYWORDS AND/OR ABSTRACT contained “REMOTE SENSING” AND “SOIL” and FRANCE in the KEYWORDS or TITLE or ABSTRACTS or at least in the address of an author. Note that we complemented this search with other expert-based searches, notably for authors who published mainly in French (not included in the WOS), or French researchers whose address was not in France at certain periods. Second, we manually excluded articles that were clearly out of the scope of our searches. Finally, we grouped together some similar keywords when their meaning was comparable.

The soil moisture retrieved by passive or active MW instruments corresponds to surface SM (1 to 5 cm in depth). Several studies have shown that root zone soil moisture (RZSM) can be inferred from time series of surface SM based on model assimilation or from simple temporal filtering methods [165].

Optical and thermal infrared (TIR) observations can also be used to map surface SM at high spatial resolution, but to date, the research is not sufficiently mature and no operational RS product exists [45,166–168]. Surface temperature measured by TIR sensors is related to evapotranspiration and can be used to estimate RZSM [169,170]. SM is an important parameter in itself, but it can also be used to estimate permanent soil properties. For example, temporal variations in SM can be used, through assimilation, to retrieve soil parameters such as soil hydraulic properties [134].

Soil roughness is an important characteristic that plays a key role in understanding/modeling different processes (e.g., slaking, runoff, infiltration, and erosion). It also has an important effect on the remote sensing signatures observed by satellites: it can be estimated because it is a parameter of interest in itself, or because its effects need to be corrected for a better estimation of other variables of interest (such as SM in the MW domain).

Soil roughness, or micro-topography, is an important influencing factor on the soil spectral response to a degree similar to that of “chromophores” [65], and is therefore a key parameter in modeling soil surface reflectance [56]. In addition, it is an indicator of the water infiltration potential, soil slaking, and erosion risk [98,171]. Several methods have been designed to measure soil surface roughness. Their main disadvantages were the time-consuming and tedious nature of the measurement in the field. Bretar et al. [172] and later Gilliot et al. [173] developed an easy-to-handle and fully automatic photogrammetric method to derive digital elevation models (DEMs) of the soil surface with millimeter resolution from multi-angular photographs captured in the field.

In the active MW domain, soil roughness has a significant effect that must be corrected to estimate other parameters of interest, such as SM and VOD. In the passive MW domain, soil roughness contributes to increased MW emissions from the soil. It is related to both micro-scale (~1 cm) and macro-scale (~100 m) topographic effects. The first global map of the observed roughness parameter from SMOS was produced by Parrens et al. [174]. The new generation of freely available radar sensors (e.g., Sentinel-1 since 2015) allows the scientific community to collect images with a revisit time (<6 days) and spatial resolution (~10 m) suitable for hydrological and agronomic applications, on local or regional scales [164]. At these scales, soil roughness mapping is mainly performed on bare agricultural soils. The radar signal increases with the roughness (root mean surface height, RMSH) according to an exponential law and becomes constant after a certain roughness threshold. Several studies show a faster saturation of the radar signal with the soil roughness when the wavelength and/or the incidence angle is small [93,175].

The third most important soil property is primarily related to soil organic carbon (SOC). This is not surprising considering that soils are the largest terrestrial organic C stocks and the question of their role in climate mitigation and adaptation is a hot topic [176–179]. Reviews on SOC mapping using RS are recent [180,181], especially using satellites [181]. Most studies rely on observation in the solar domain, at scales ranging from the field to regional, and finally, to national or even transnational scales. Most approaches have been conducted on bare, cultivated soils: the higher the scale, the lower the accuracy. The prediction performance varies according to the type of soil [123], the date of acquisition [182], and the presence of crop residues on the surface [22,183]. As far as French research is concerned, RS studies have been conducted at local or regional scales and none of them have yet specifically addressed the use of RS at the national scale of metropolitan France. Studies at smaller scales have mainly relied on UAVs [173] and airborne imagery [184] at a very high spatial resolution ( $\leq 2.5$  m), while at larger scales, most studies have relied on high-resolution satellite images: Hyperion [185], SPOT [186,187], Sentinel-2 [123,182], and/or Sentinel-2 with the joint use of Sentinel-1 [128,129]. The accuracies found for mainland France range from  $2 \text{ g kg}^{-1}$  to  $6 \text{ g kg}^{-1}$ , leaving open the feasibility of monitoring SOC according to agricultural C-stocking practices. This feasibility, especially the influence of the composition of the soil surface, is the subject of studies at the French and European levels.

Soil color is an important soil property that is directly related to the reflectance of soil in the visible [46,51,80], which depends mainly on the so-called “chromophores” [108]: soil organic carbon content, Fe sesquioxides, calcareous content, moisture, and to a lesser extent, soil texture and mineralogy. It is widely used in conventional mapping and soil taxonomy. The Munsell color coordinate system was related to visible bands by R. Escadafal [46,80], resulting in the cluster diagram of soil lines versus Munsell color. In our literature database, it was not always easy to distinguish soil color from soil brightness and soil albedo. While the term “soil color” is often used in soil science, the RS community that focuses on vegetation monitoring has investigated color-related soil surface properties such as soil brightness derived from the soil line concept or soil albedo, mainly derived from inversion of kernel-driven reflectance models on selected directional reflectance data [188].

Topsoil texture defined as the relative proportion of clay, silt, and sand is one of the most important characteristics of soils. It determines many of their physical and chemical properties and behaviors (e.g., water retention, mechanical behavior, infiltration capacity,

nutrient and pollutant concentrations, friability, and trafficability). Attempts to map soil texture have shown that the best results were achieved in the visible, near infrared, and shortwave infrared from hyperspectral airborne images (e.g., [124,126,189,190]) or from multispectral satellite images [130,191–193]. These works have mainly focused on clay texture and/or clay content estimation due to the specific absorption of clay minerals around 2200 nm [194]. As observed for SOC estimation, the texture prediction performance of topsoil varies with the date of acquisition and the presence of crop residues on the surface [193].

Finally, in the early stages of the use of RS for soil mapping, RS was often used to delineate/identify soil types or soil classes (e.g., [61,63–73,75,76,195]). At the initiative of French geographers, in particular E. de Martonne [196], these approaches were initially based on the visual interpretation of aerial photographs, most often in photogrammetric mode for a better identification of morphological units [26–28]. We can introduce here the notion of soilscape, defined as “a landscape unit including a limited number of soil classes that are geographically distributed according to an identifiable pattern” [197]. A spatial layer of the soil factor can then be analyzed in terms of such identifiable patterns. Digital processing of single-date raster images using a per-pixel classifier [75,195,198] or “textural analysis” [74,76] has been proposed to mimic and replace visual interpretation. Some approaches have used digital clustering of soil profile data [199], through the DIMITRI algorithm [61,200] or hierarchical clustering [72] of semantic information about soil map units. The DIMITRI algorithm was later incorporated into the OASIS algorithm [201], whose objective is to identify repeated patterns in the image by calculating the “composition or class frequency vector” of a given square neighborhood in the image. A similar approach has been developed using the CLAPAS (*CLAssement des PAysages et Segmentation*) algorithm proposed by J.M. Robbez-Masson [202,203]. The main soilscales of Lebanon were derived from a single-date Landsat image using OASIS [76], while SPOT was used to obtain large vineyard units in the southern Rhone Valley [74]. First applied to non-spectral data [197,204], CLAPAS was then applied to a MODIS time series at four dates to map the main landscape units of Brittany [205,206]. Pixel-based approaches have been especially applied in contexts where the soil is often bare, as in arid environments [195,198] or on Mediterranean vineyards with bare inter-rows [75]. In addition, a pixel-based approach relying on both a SPOT time series and morphometric layers (elevation and derivatives) to map South African terroirs was a step toward DSM formalism. It performed bootstrap selection of the training/validation areas in order to implement regression trees, and then a “Hyperstat” algorithm calculated the modal value in the output map stack and the assignment frequency as an indicator of mapping uncertainty [77].

Figure 2 shows the temporal evolution of the number of articles by soil properties. This trend relates to technological advances (new satellites and sensors) and scientific and political interest in specific soil properties. We observe a remarkable increase for all properties between the late 1990s and the early 2000s. This is likely due to the launch of Landsat 7 and its Enhanced Thematic Mapper Plus (ETM+) sensor, which allowed for more accurate assessments of the land surface [24]. In 2008, the United States Geological Survey (USGS) made all Landsat 7 data available to the public [207], and even free in 2009, which led to a large increase in downloads and probably explains the largest increase in publications after 2010. Studies on some soil properties have steadily increased (i.e., soil moisture), while some seem to have had a rather constant interest over the last twenty years (roughness, temperature, color, and albedo). In particular, although almost absent in 2007, SOC shows a strong increase in interest. This increase is arguably related both to the growing interest in SOC, especially driven by the IPCC [208], and to the launch of satellites that better capture a wide range of SOC-related spectral bands (e.g., [209,210]). Despite their relatively smaller numbers, soil texture studies show a notable increase that is also related to technological advances (imaging spectroscopy (e.g., [124,126])).



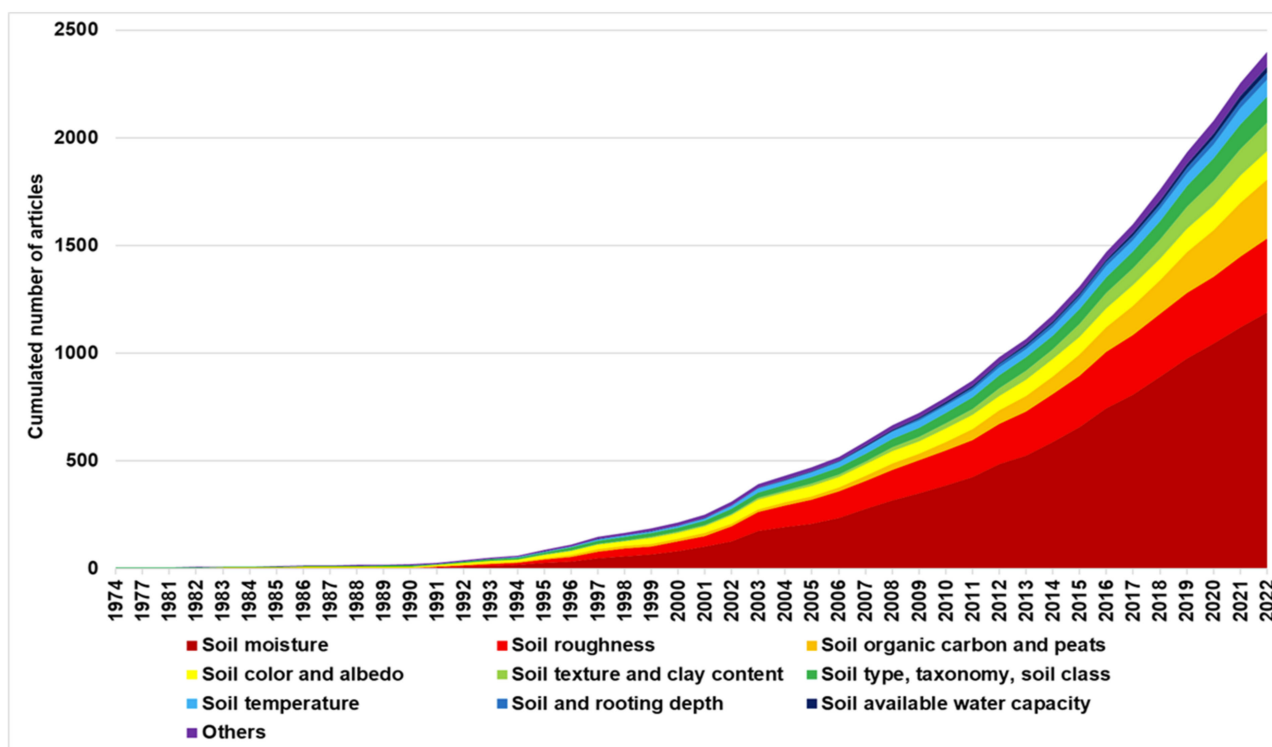


**Figure 2.** Evolution of the cumulative number of articles per soil property.

### 3.3. Trends in French Remote Sensing Research in Relation to Threats to Soil

In this section, we focus on articles that explicitly mention soil threats in our corpus of publications (Figure 1). Soil threats are classified according to the proposals made by the EU Soil Thematic Strategy [9,211] and the EU soil strategy for 2030 [10]. The relative importance of soil threats (Figure 3) is related both to their importance in the political agenda and to the feasibility of using RS products to monitor these threats.

The strong dominance of SOC is clearly related to the feasibility of reporting, monitoring, and verifying soil carbon stocks according to article 3.4. of the Kyoto Protocol (e.g., [212,213]). It also links to the COP21 Paris Agreement and the four per Mille initiative [177,214,215]. In addition to advances in temporal frequency, high spatial and spectral resolution RS imagery offers an unprecedented opportunity to study and monitor the spatiotemporal dynamics of SOC changes [111,181].

The second threat is the sealing of soils by urbanization, industrialization, road construction, etc. It corresponds to an almost irreversible loss of many soil functions and is particularly widespread in some regions of France (mainly peri-urban and coastal areas). The fine spatial resolution of the new RS sensors enables them to monitor the expansion of sealed areas over time. In France, the Land Cover Scientific Expertise Center (CES OSO, <https://www.theia-land.fr/> accessed on 29 May 2023) automatically produces land-cover maps for metropolitan France from Sentinel-2A and Sentinel-2B data. These maps have a ground sampling distance (GSD) of 10 m. They are used to monitor the rate of soil sealing and/or to take into account the services rendered by soils in land-use planning (e.g., [216–218]).

The third threat is erosion, which is a serious problem in French agricultural soils (e.g., [219–221]). Soil crusting and slaking have been studied using RS for a long time (e.g., [98,222]). High-resolution imagery is an increasingly used technology for mapping erosion [223]. Soil surface changes can also be captured by DEM series from UAVs [224].

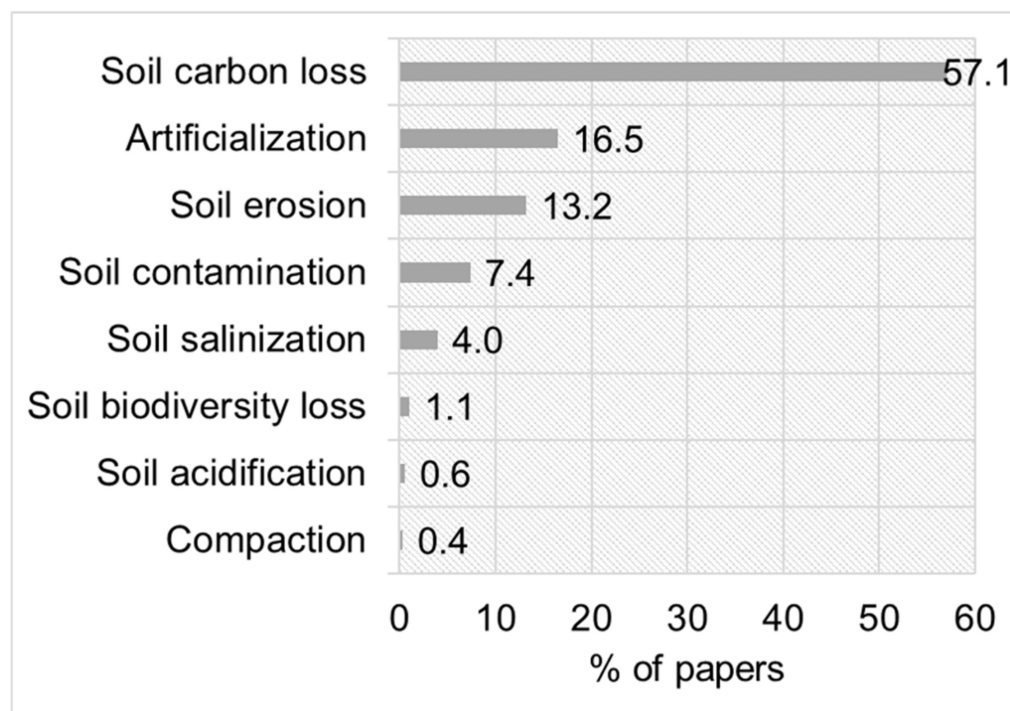


**Figure 3.** Percentage of articles per soil threat (out of 857 articles where threats were explicitly mentioned).

Examples of soil contamination are less numerous, often related to the impact of mining or industrial activities on trace elements (e.g., [225,226]), hydrocarbon and oil contamination (e.g., [227–229]), and some radionuclides [230]. Many studies are still based on hyperspectral, fluorescence, or photoluminescence measurements performed in the laboratory or by proximal RS (e.g., [226,231]). There are, however, a few studies using airborne hyperspectral or gamma-ray spectrometry data [227,228,230,232–235].

The fifth most important threat is soil salinization, which is a very serious problem for soil fertility. It mainly concerns arid and semi-arid regions and is often linked to the quality of irrigation water [4]. Mainland France is not a salinization hot spot, except for a few local areas such as the Rhone delta (Camargue). However, French research is very active in the field of soil salinization RS. This is partly due to the history of France and its relationships with certain countries. This is also related to the fact that salinization crusts are quite easily detectable, even in the visible, and that studies on soil salinity mapping and monitoring have been developing for a long time and are still ongoing (e.g., [99,101,198,236,237]).

Other soil threats are more rarely studied using RS. Biodiversity, compaction, and acidification are not directly related to RS imagery. Indicators of soil biodiversity or acidification can, however, be captured by RS through vegetation or land use. In this case, they are often combined with other covariates in DSM tools.

Figure 4 shows the evolution of the cumulative number of articles per soil threat.

The most striking trend is the almost exponential number of articles on soil carbon loss. As explained above, this trend relates to both policy issues and advances in the feasibility of monitoring SOC. Similarly, we observe a large increase in soil sealing studies, related to population growth, soil sealing, and land-use issues, as well as the opportunities provided by new high-resolution, time–frequency satellites. The increase in soil erosion and contamination studies also relates to global issues and advances offered by new sensors. In comparison, studies on soil salinization remain rather stable; biodiversity is slowly emerging, while acidification and compaction are almost negligible.

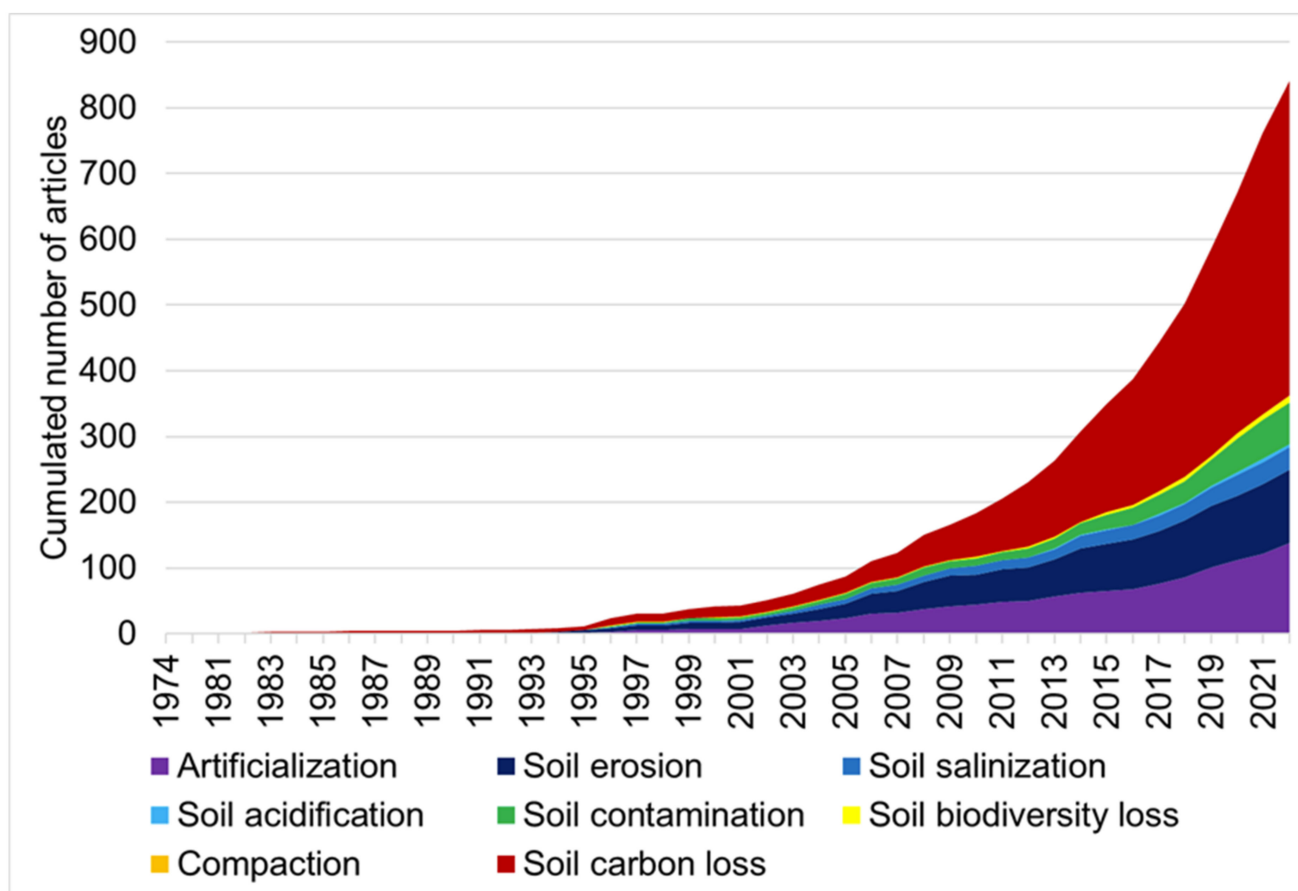


**Figure 4.** Evolution of the cumulative number of articles per soil threat.

### 3.4. Remote Sensing of Soil Properties as Training Data for Digital Soil Mapping

Similar to laboratory measurements, RS predictions can be used as an “s” factor in the SCORPAN model (i.e., they are used as if they were “measurements” of the variable of interest). In this case, the main challenge is to incorporate the uncertainties associated with these inputs into the SCORPAN model. Note that this issue also applies to laboratory measurements, although it can be assumed that they are generally more accurate than those derived from RS data. Another important limitation of using RS data as direct inputs to calibrate DSM models is that soil reflectance only captures information about the surface layer, while soils are 3D objects. Only radar or gamma-ray spectrometry techniques are capable of observing a soil at depth.

If the prediction does not include a spatial component, and if there are a sufficient number of validation points, an easy and often-used way to verify the absence of a spatial component is to perform geostatistical analyses on the prediction residuals. If there is a spatial structure on the residuals, it is possible to improve the predictions by kriging or find that this trend might be related to another covariate that could be incorporated in a SCORPAN model.

It is important to keep in mind the consequences of uncertainty if these predictions are not only used to predict a value at a given time, but also intend to monitor changes in a soil characteristic. First, cumulative errors at two dates will affect the minimum detectable change (i.e., [238]). Second, it is debatable whether it is better to map soil attribute values at two dates and then infer changes from their differences, or whether it is better to directly map the changes themselves. Both from a spatial and soil process point of view, the spatial structures and controlling factors of a soil attribute at two different dates may not be the same as the changes between two dates. It should be noted that the above remarks are relevant to both for the “direct RS detection of soil properties” and DSM.

#### 4. Incorporating RS as Covariates in DSM

##### 4.1. Soil Property Maps Using Remote Sensing on Bare Soils as Covariates in DSM

Instead of using the soil spectral response to inverse a model prediction of a soil property, an alternative is to incorporate the map of that prediction as a covariate in a SCORPAN model [239–241]. These studies are limited by the spatial availability of bare soil images; the influence of perturbing factors such as soil roughness [157], moisture, and vegetation residues on the topsoil [102,242]; mismatches between soil sampling and remote sensing acquisition dates (e.g., [186]); and, in some cases, the low variability and range of some soil property values [123,126,182]. Increasing the frequency of acquisition dates (e.g., with S1 and S2 products) now enables the detection of more bare soil fields and area expansion by mosaicking several images [128] and reduces the influence of soil moisture and crop residues on the prediction accuracy (e.g., [128,129]). Figure 5, extracted from [243], shows an example of RS data on bare soil used as covariates in a DSM model to predict SOC in a region of central France. Interestingly, the covariates derived from RS imagery on bare soil are among the most important in SOC prediction.

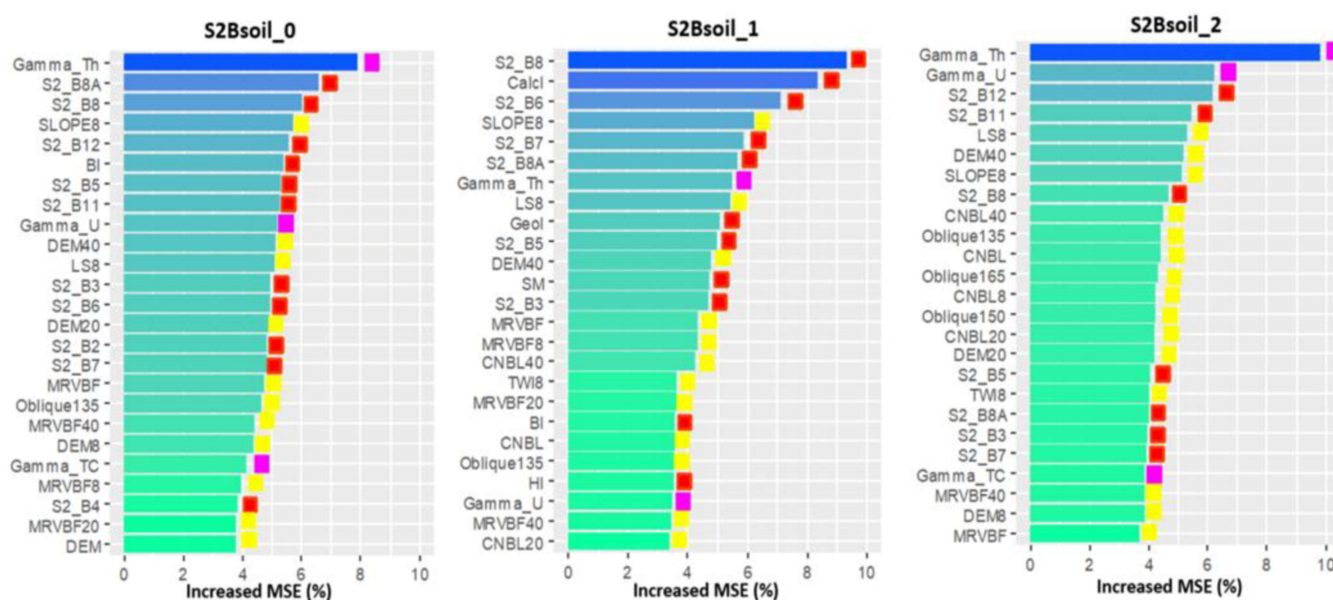


**Figure 5.** Relative importance of the first 25 environmental covariates for SOC prediction by DSM in the Beauce region (France) using different learning soil data and incorporating RS data among the covariates. The color palette (light green to blue) indicates the degree of importance of the covariates; the least important covariates are in light green and the most influential covariates are in blue. The red squares are data derived from Sentinel 2 spectral bands; the pink squares are airborne gamma spectrometry maps; the yellow squares are other environmental covariates. Adapted from Urbina-Salazar et al., Remote Sensing, 2003, 15, 2410, Figure 5.

In this example, the question of how to combine these soil predictions with a model adapted to usually vegetated areas remains to be solved, in order to obtain a full DSM map of soil properties over a large area including various land uses. This general question applies for nearly all RS data obtained from bare soils. If one wishes a full map of a landscape, RS data on bare soils are almost never available on the whole area, except for deserts.

##### 4.2. Remote Sensing Data as Proxies of Soil Properties Controlling Factors in the SCORPAN DSM Model

###### 4.2.1. Climate

On a global scale, climate is one of the major controlling factors for weathering and subsequent pedogenesis. Actually, the birth of pedology relates to Dokutchayev's pioneering

work on the zonal climatic distribution of soil types in Russia (e.g., [244–247]). At this scale, climate is also the major controlling factor for SOC contents and stocks (e.g., [177,248]), either through the effect of climate on vegetation-derived SOC inputs (e.g., in the hottest and driest regions) or through the effect of very low temperatures on lowering the rate of SOM mineralization (e.g., in the circumpolar and high-elevation regions).

Figure 6 illustrates the global effect of climate on the world's carbon stock distribution downloaded from the website <https://soilgrids.org/> accessed on 29 May 2023. The original work on DSM at the global scale is from Poggio et al. [249]. As explained in this article, climate is one of the most important driving factor of SOC stocks at the global scale. The map clearly highlights the effect of temperature in the Northern latitudes and in the mountains. There is also an effect of a very wet and hot climate, for example, in Indonesia.

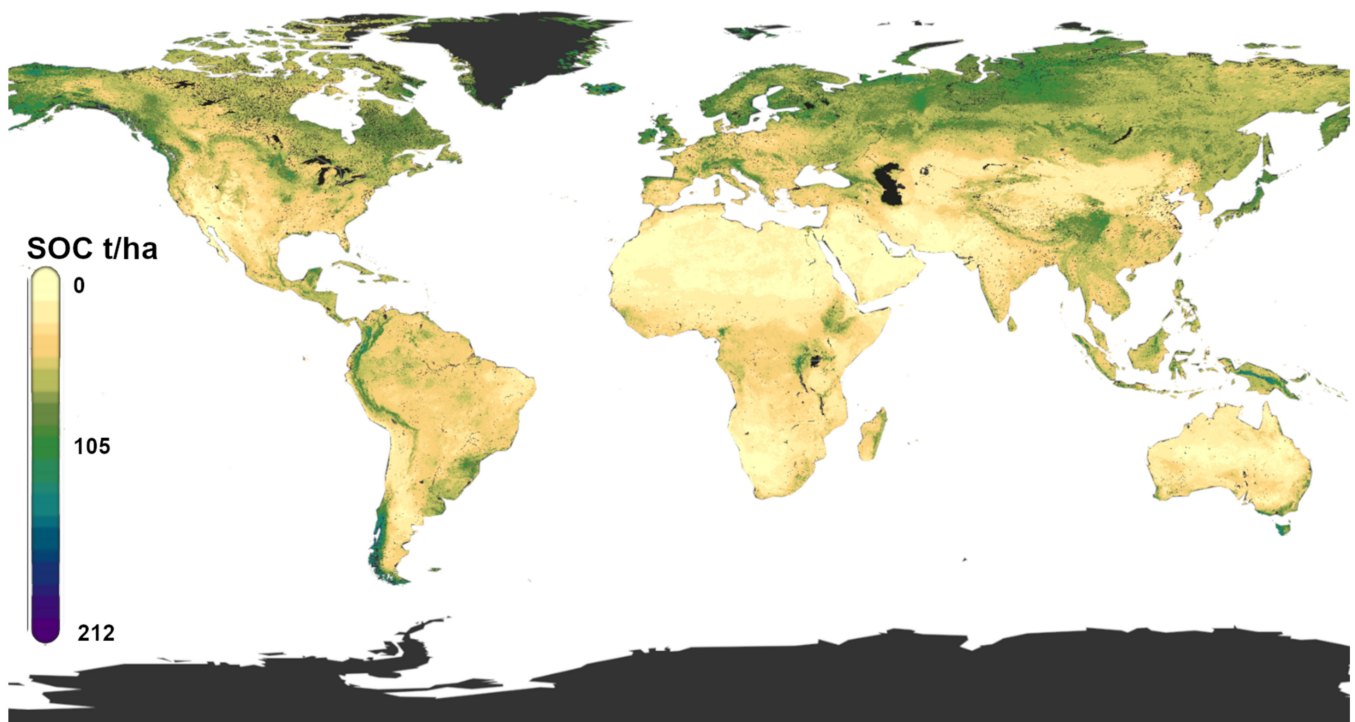


**Figure 6.** Global DSM map of SOC carbon stocks. Adapted from an image downloaded from <https://soilgrids.org/> accessed on 29 May 2023—© ISRIC-World Soil Information, from the original work by Poggio et al. [249].

At the scale of mainland France, latitude and altitude are clearly the two main controlling factors for SOC, together with land cover (e.g., [250–252]). The effect of altitude was also demonstrated for climatic gradients related to elevation or rainfall in smaller regions (e.g., [238,253,254]).

Rainfall intensity is another major controlling factor for soil weathering [255] and erosion [256]. Finally, climate change is one of the factors accelerating certain pedogenic processes and threats to soil [4].

#### 4.2.2. Land-Cover and Vegetation Characteristics

Land-cover classification based on RS products is a relevant covariate for predicting many soil attributes, in particular SOC. In mainland France, studies have used land-cover maps as covariates to map SOC concentrations or stocks (e.g., [138,250,257–259]). Land-cover classification from RS products can be a relevant covariate for predicting many soil attributes. Other studies have also shown that SOC sequestration potential was also related to land cover (e.g., [216,260,261]). Land cover is also clearly related to soil pH as well as parent material [259]. RS products are one of the main tools used for assessing human

pressure on soil contamination through the distance to urban or industrial areas and major roads (e.g., [262–264]).

Changes in land cover (and the transition duration from one land cover to another) are also direct controlling factors of erosion risks. In a review paper, King et al. [222] summarized soil erosion monitoring and modeling from RS. The first interesting piece of information accessible via RS is vegetation cover, as bare soils are generally the areas that contribute most to runoff (e.g., [265–267]). RS has also been used as an indicator of slaking [268]. Hill et al. [269] monitored land degradation, soil erosion, and desertification in a French Mediterranean region and demonstrated excellent accuracy in identifying soil degradation levels using airborne imaging spectroscopy (AVIRIS) and Landsat TM data. For erosion as well, the distributions of land use across the landscape and connectivity between fields are studied using RS and provide useful information on runoff concentration risks [270,271]. RS information on soil roughness, for example using radar data, can also significantly improve erosion prediction and modeling [93,222].

Finally, land cover may sometimes be correlated to some specific local soil properties. For example, in large, cultivated plains such as the Beauce region in France, small, forested plots are often related to very shallow soils [272].

The identification of bare soils uses vegetation indexes such as NDVI (Normalized Difference Vegetation Index). These were designed to assess the amount of green vegetation [273]. As such, they can also be used as proxies of organic carbon inputs to the soil when integrated over rather long periods of time (e.g., monthly or annual averages, [259,260]). In this case, the amount of green vegetation is supposed to be related to the carbon originating from roots and/or crop residues.

Vegetation indexes, such as land surface temperature (LST), as evapotranspiration factors, can also be an indicator of vegetation stress and the soil's available water capacity (AWC) for plants during dry periods [274–276]. In general, the AWC can be calculated using pedotransfer functions (PTFs), established between water retention characteristics and some other spatialized information (e.g., texture, depth or rooting depth, bulk density, and coarse elements, [277,278]). Another way to obtain indirect information about the AWC is to assimilate RS data into vegetation functioning models (e.g., [279–281]). Fusion approaches have also been developed to combine local soil property measurements with RS data [282–284]. A recent review by Cousin et al. [285] provides an insightful overview of the ways to estimate the AWC using RS data as covariates for DSM AWC prediction from field to regional scales.

#### 4.2.3. Relief, Topography, and Landforms

Relief, topography, and landforms are among the main controlling factors in the SCORPAN model [11,286]. The covariates used in DSM are generally computed derivatives of Digital Elevation Models (DEMs). For global mapping, Sanchez et al. [287] and Arrouays et al. [286] recommended using the Shuttle Radar Topographic Mission (SRTM) DEM at 90 m resolution. The main reason for recommending SRTM was its availability and reasonable resolution considering the number of pixels generated (about 18 billions). Of course, there are now more accurate DEMs available from other RS products, including Lidar for the most accurate ones (e.g., [288,289]). DEM derivatives have proven to be very efficient as covariates in DSM at different resolutions and area sizes, from field to national scales in France (e.g., [138–140,144,145,259,272,290–293]). The integration of DEM derivatives at various resolutions has also proven to be useful in capturing different scales of variability (e.g., [141,144,272]). Note that in some cases, elevation replaces temperature or rainfall/snowfall. It is clear that relief attributes directly reflect or control many factors in soil evolution (e.g., temperature, slope, soil depth, erosion and deposition, and alluvial plains). Conversely, some changes in soil surface topography can be useful covariates to help detect rill erosion [224], landslides [294,295], or the swelling/shrinkage of clay soils (e.g., [194,296,297]).

Note that, although French examples are not dominant in the literature (e.g., [76,129,144,201,202]), the automatic classification of landforms from DEM and other satellite imagery is one of the classical foundations of spatial segmentation, which is a technique often used for large-scale DSM (e.g., [142,298–301]).

#### 4.2.4. Parent Material

Historically, information about parent material in DSM came primarily from digitizing geological or lithological maps, or soil maps in which the parent materials were described. This is still the case for many studies. However, RS products have proven their ability to detect and map certain parent materials through the spectral signature of outcrops, regolith, or upper soil, especially using airborne gamma-ray spectrometry. This has been shown in France in a large number of situations (e.g., [135,141,232,272,302–305]). Figure 7 shows four DSM predictions of topsoil texture [305] in a French department, using a large set of covariates and then adding a lithology map, or a gamma-ray spectrometry map, or both. It shows that gamma ray spectrometry captures some rather large spatial patterns linked to the parent material that were not captured by the lithological map.

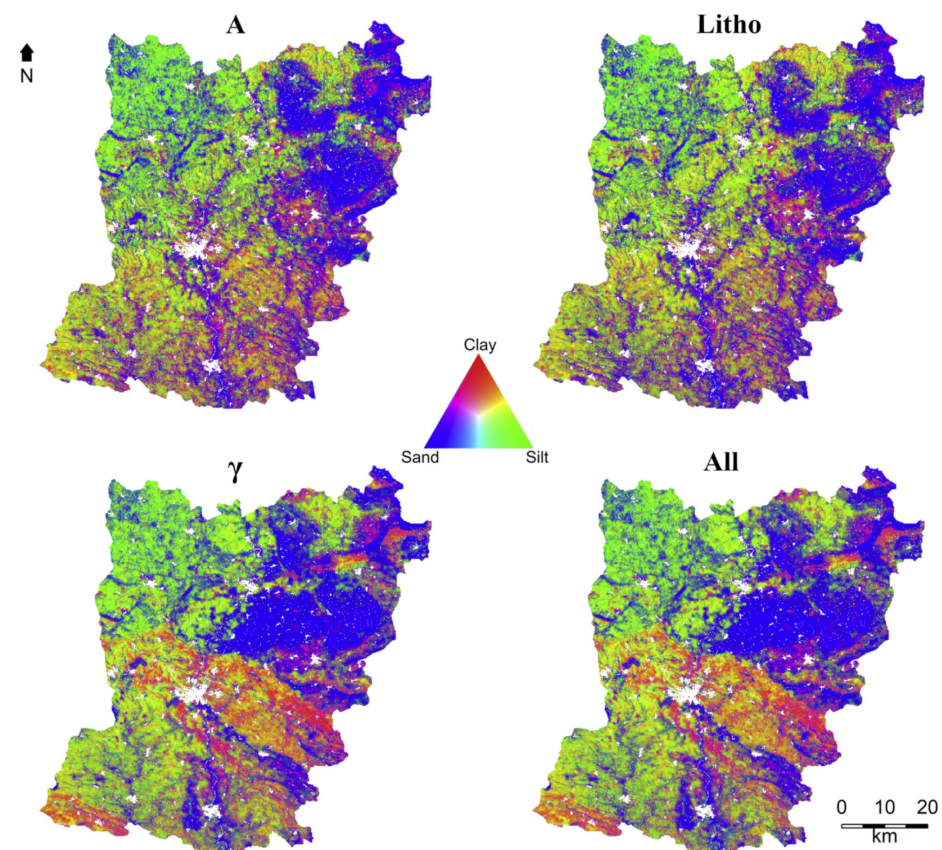


**Figure 7.** Red/green/blue composite of predicted soil textures (clay/silt/sand in g/kg) for the topsoil layer in the Mayenne department (France). White areas are cities. Comparison of DSM predictions using the following: (A): a set of covariates without incorporating lithology or gamma-ray spectrometry maps; (Litho): the set A plus a lithology conventional map, ( $\gamma$ ): the set A plus gamma-ray spectrometry maps; (all): all covariates. Extracted from Loiseau et al. [305]. This article was published in *Geoderma Regional*, 22, Loiseau T., Richer-de-Forges A., Martelet G., Bialkowi A., Nehlig P., Arrouays D., Could airborne gamma spectrometric data replace lithological maps as co-variables for digital soil mapping of topsoil particle-size distribution? A case study in Western France. 22, 1-15, e00295, 2020, doi:10.1016/j.geodrs.2020.e00295. (Figure 12, page 13 in [305]) with permission from Elsevier®. Copyright Elsevier (2020).

Applications of RS to detect typical parent materials or mineralogy are quite common in tropical environments (e.g., [109,306]).

#### 4.2.5. Age

According to Chen et al. [21], age is the least-used covariate for medium- and large-scale DSM. It is a rather complicated covariate to interpret because it mixes the duration of weathering and pedogenesis (both its duration and the various climatic and vegetation conditions in which soil formation occurred). Overall, age is quite difficult to infer directly from RS data. Where soils have developed from the underlying parent material, the age can be inferred from lithological or geological information (see Section 4.2.4). However, to our knowledge, there are no RS sensors that are capable of capturing age at the pedogenesis time span. For shorter periods, time can be captured through land-cover change history or other types of measurements. Although we did not find any soil studies using gamma-ray spectrometry or other tools to measure the erosion/sedimentation rates in French soils, some works suggest that this technique may have potential for detecting change related to nuclear accidents (e.g., [307,308]).

#### 4.2.6. Soil Management Practices

In the “o” factor or the SCORPAN model, all organisms are included, although in most cases, “o” is represented only by vegetation indexes or biomass-related vegetation characteristics such as NPP. Among the organisms that have a major effect on soil properties and changes, one of them is obviously humans, through their impact on soil management practices. We refer here to a recent review by Bégué et al. [309], which emphasizes that the potential of RS to characterize cropping practices is not yet optimal, and that the new generation of high-resolution sensors (space, wavelength, and time) should allow for the improved characterization of cropping practices. In another review, Bégué et al. [310] stated that “less than 10% of the publications on remote sensing and agriculture actually focused on cropping practices” in the previous decade. In their 2018 review, they distinguished between three broad groups of cropping practices ([309], Figure 1):

1. Crop succession (i.e., the sequence of crops or fallows in consecutive years at the field scale);
2. Cropping patterns (e.g., temporal sequence and spatial arrangement of crop, fallows, and landscape features in a particular land area);
3. Cropping techniques (e.g., irrigation, organic amendment, crop residue management, tillage, harvesting, duration of bare soil, grazing of moving cattle feed, and implemented on a piece of land).

It is beyond the scope of this study to detail all the sensors, indices, and data they listed in their review to detect all these soil management practices. Figure 8 shows the main cropping practices reviewed by Bégué et al. [309].

One of their main conclusions is “the majority of the studies are exploratory investigations, tested at a local scale with a high dependence on ground data, involving one remote sensing sensor at a time, and are constrained by local knowledge and conditions”. However, they pointed out the high potential related to the increasing availability of RS data suitable for fine resolution and time-scale monitoring (e.g., Sentinel 1 and 2, hyperspectral sensors, Lidar) and the combination of different satellite sensors [311,312]. Research should therefore be conducted to better map these soil management practices. One of the major difficulties was obviously related to the low spectral, spatial, and time resolution. Another outstanding question is what type of information derived from RS should be considered as a covariate for DSM? There is probably not a universal answer to this question; it may depend on the case, area, or soil property.



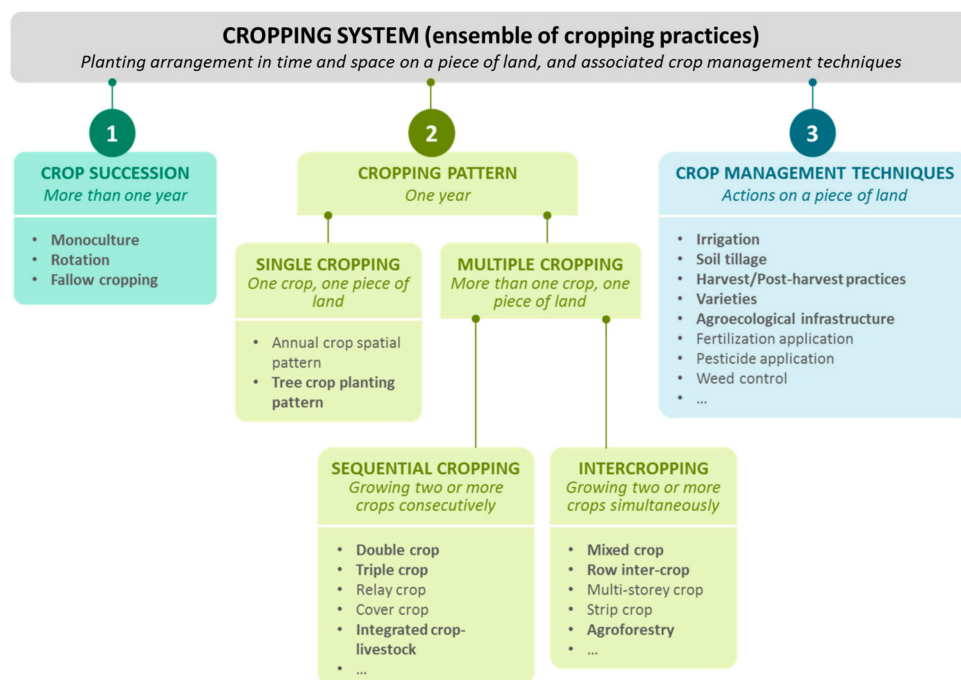


**Figure 8.** Main cropping practices accessible via remote sensing and reviewed by Bégué et al. [309]. After Bégué et al., Remote Sensing and Cropping Practices: A Review. *Remote Sensing* **2018**, *10*, doi:10.3390/rs10010099. Bold cropping systems were reviewed. © Bégué et al. with permission of the authors.

Nevertheless, we believe that this essential information will be incorporated into future DSM and will provide major advances in soil knowledge. First, it will better filter out some information that is often considered “noise” for some DSM predictions (e.g., soil roughness or dead vegetation residues for SOC). Second, it will provide critical information on the controlling factors of soil changes on the local and landscape scales. Such quantified information may include, but is not limited to, crop rotation [179], grassland management [313], spatial arrangement of crops and land use, linear features such as hedges or drips [314], soil water regimes and their consequences on SOC inputs and salinization, etc. Indeed, a large field of research is still open in order to find the right RS soil management and cropping practices to incorporate in the DSM covariates. A major difficulty could be the diversity of situations in which we will approach large-scale studies. A preliminary large-scale delineation of “agrarian” regions could be a solution, as suggested by Bellon et al. [315]. Furthermore, this typically “multi-scale” RS challenge may benefit from data fusion of different RS data at different wavelengths, resolutions, and revisit periods.

Finally, from the perspective of local soil management and security, this is really crucial, because it can fill the gap between DSM and local farmers and actors, as crop and soil management practices are indeed, a very local way that farmers can try to improve soil conditions [316,317].

## 5. Use of Remote Sensing to Design the Sampling Strategy for DSM

When RS products are available and relevant in a target area, and if we assume that the SCORPAN model for DSM is efficient, it seems logical to optimize the soil sampling design based on covariate space, and thus to use for designing the sampling, RS products alone or with other covariates. This may be especially useful if the number of soil measurements/observations is constrained. This has led some authors to propose that soil sampling is designed in terms of covariate space. One of the seminal articles in this technique is the constrained Latin Hypercube Sampling (cLHS) proposed by Minasny and McBratney [318].

The cLHS sampling in the presence of covariates is designed to select a limited number of sites in an area.

According to Minasny and McBratney [318], “This kind of sampling should produce a reasonably efficient way of sampling soil and its environment so that the range of conditions are encountered, ensuring a good chance of fitting relationships if they exist”. The last words of this quote, i.e., “if they exist”, are very important to consider. A strong assumption of cLHS is that the selected covariates represent the variability of the target variable. In other words, if a controlling variable is missing from the set of covariates, the sampling design has a high probability of missing part of the variability of the target property.

The main advantage is to optimize the number of samples and thus the sampling effort and cost to capture the main combinations of the covariate feature space. One of its weaknesses is that it is not well suited to some spatial modeling techniques, such as geostatistics and kriging [131]. This is because cLHS, in its process of selecting sampling points, maximizes the feature difference between sampling points. The residuals of the predictions obtained after modeling using a cLHS sampling for calibration, can, however, be analyzed by geostatistics or other validation techniques, on the condition that an independent validation set is available (see an example in Figure 9, left). Note that in the figure extracted from Minasny and McBratney [318], they just use the stratified sampling design as an example compared to cLHS.

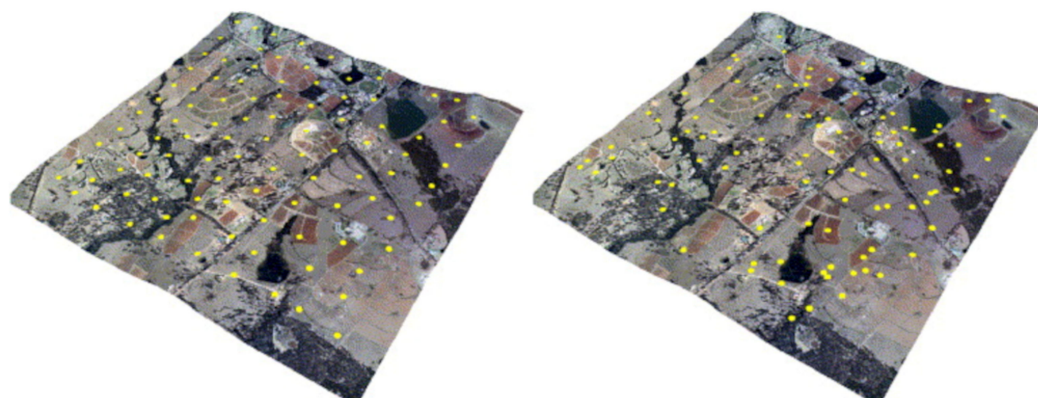


**Figure 9.** Example of the location of sample points in landscape using stratified random sampling (left) or using cLHS (right). Extracted from Minasny and McBratney [318]. *Computers and Geo-Sciences*, 2006, 32, 1378–1388, doi:10.1016/j.cageo.2005.12.009. Figure 5. Reprinted from *Computers and GeoSciences*, 32, Minasny B. and McBratney A.B., A conditioned Latin hypercube method for sampling in the presence of ancillary information, 1378–1388, Copyright (2006), with permission from Elsevier, License agreement n° 5556000526726.

Various adaptations of cLHS proposed by different researchers consider accessibility and cost, or better space filling (e.g., [319–321]). Space filling has the advantage of not missing situations that could be under-represented by cLHS. If, for example, a large area is characterized by similar combinations in the feature space, it might be under-sampled, even if it contains a soil variability that is not captured by the covariates. Wadoux et al. [322] recently studied sampling design optimization for soil mapping with random forest, and concluded that cLHS sampling performed worse than other sampling designs. It should be noted that, in their study, the subsampling design was based on a preliminary selection of an existing set of sample sites that was already a mixed sampling design, i.e., subsampling a regular grid using a method close to cLHS, and with known results (LUCAS Soil, [323]). In other words, the spatial coverage of their learning full sample was already rather efficient, and some covariates had already been used to locate the samples in the grid.

Note that the idea of exploring the cLHS method using covariates on a dense set of already sampled points was also tested by Loiseau et al. [141], who concluded that it was efficient at highlighting situations that were under-sampled in the original soil legacy

dataset. Briefly, they tried to predict topsoil particle size distribution using various DSM techniques and a set of covariates. When applying cLHS to the covariates, they found that the initial dataset missed some covariates combinations, which explained why some areas had a bigger uncertainty, or even a bias, in the predictions.

Another interesting characteristic of direct RS prediction is that it can be used as a dataset to simulate the spatial distribution of a soil property and thus be used to simulate different validation sampling strategies in spatial or feature space (i.e., [132]) and highlight their advantages and limitations. This kind of direct prediction, if accurate enough, can also help test different sampling strategies for the training dataset. This test on sampling strategies was conducted by Lagacherie et al. [131] in order to assess their impact on the accuracy of the prediction of topsoil clay content in Tunisia. In particular, they showed that stratified random sampling, which is often recommended for soil map validation [137], could lead to inconsistent results if the number of strata and/or the number of random samples taken in each strata were not large enough. For a recent synthesis about sampling in DSM, see Brus [137].

## 6. Limitations and Challenges

In this section, we focus on the main limitations of RS products for soil mapping and monitoring and some challenges to improving the quality and relevance of RS imagery for soil.

### 6.1. Using RS Products to Predict Soil Properties

The use of RS measurements as a substitute for soil analyses is a way to increase the density of soil information at a low cost. However, this surrogate often remains difficult to obtain with satisfactory accuracy and broad spatial coverage. With respect to accuracy, work remains to be conducted to better distinguish the effects of different factors on the spectral response of a soil property. A typical example can be taken for mapping SOC using the spectral signature of bare soil. A large number of limitations include, for example, the following:

- How do we discriminate bare soil from vegetated soil, e.g., what NDVI threshold should we use? Which unmixing method should we use for partly vegetated pixels?
- How do we distinguish bare soil from soil covered with dead vegetation residues? Additionally, what threshold should we use?
- How do we take into account the complex effects of different soil properties at a given time/location (e.g., vegetation, residues, moisture, roughness, SOC, and clay or lime content)?
- How do we extend the coverage of bare soils? Mosaicking is now well developed, but what time period should we take? What are the limitations related to mosaicking? How can we take into account the fact that different dates are usually associated with different situational conditions (e.g., moisture and roughness)?
- In many cropped regions, more and more soil will no longer be bare due to the implementation of cover crops and/or seeding under a vegetative cover.
- How do we take advantage of various RS products and sensors, depending on their resolution (in space, time, and spectral domain), remoteness and related perturbing factors?
- At the field or farm-scale, responding to these questions may imply using several RS sensors. For example, using UAV RS enables the selection of the most adapted dates to obtain bare soil imagery together with minimizing the perturbing factors of soil spectral data. This is, however, not feasible for broad-scale monitoring. The effect of some perturbing factors may also be studied using airborne imagery. Thus, studies comparing laboratory spectra, proximal sensing, UAV, or airborne data to satellite imagery, should be conducted in order to estimate/reduce the errors due to changes in spectral resolution/remoteness and to improve the criteria for selecting the relevant satellites data (e.g., [324–326]).

### 6.2. Most RS Products Only Capture Topsoil Information

Almost all DSM attempts show that the prediction performance decreases with depth (e.g., [21,259]). This is easily understandable because most RS products only capture information about the soil surface and/or terrain attributes at the time of acquisition. For example, it is physically impossible to detect deep soil attributes with visible–near infrared RS data. Some products, however, have the capacity to integrate a response over a less limited depth (radar and gamma-ray). Therefore, one challenge is to better incorporate different sensors that are capable of obtaining information at different depths into the DSM framework. Other information than bare soil spectra can be useful to map soil properties at depth. Gamma-ray spectrometry data, however, comes mainly from low elevation airborne sensors, which are not yet available in many parts of the world. Magnetic surveys are most often used for detecting soil pollution (e.g., [327–329]). They may also, however, reveal lithology, weathering, and water regime of soils (e.g., [330–332]). Yet, to our knowledge, there are no studies using airborne magnetic data as covariates in DSM.

Another challenge is to integrate some soil knowledge into the DSM. For example, it is well known that in many cases, soils are organized in topo-sequences or “catenas”. This is the case of erosion catenas from a plateau to a gentle slope. At the top of the eroded portion of the catena, one can obtain information about deeper horizons present on soils developed on the plateau, as these underlying horizons may have been exposed at the surface by erosion. The same inferential information can be incorporated into DSM in the case of steep slopes, where outcrops can provide information about the parent soil material. In this case, a sampling design based on topo-sequences and available high-resolution RS imagery can be very efficient (e.g., [333]).

This type of integration of soil knowledge into the DSM is not trivial because it requires a soil scientist to know the soil spatial organization and the scales involved in order to incorporate such information into the DSM. In some cases, these rules are described in conventional soil maps, and a challenge is to take them into account to disaggregate complex soilscape map units into more precise classes (e.g., [146,147,334–336]).

Finally, a solution often chosen to address the limitations of bare soil RS and to obtain information on some deep soil properties is to incorporate other RS data, such as vegetation indices or land-cover changes, as covariates in a DSM model (see Section 4.2, and further, Section 7.2.2). At the global scale, Padarian et al. [337] recently used a semi-mechanistic model combined with an MODIS time series of changes in land cover to model changes in the global SOC stocks from 2001 to 2020. Though this approach is still not perfect, because it does not take into account climate change and some inherent soil properties, it provided an estimate of the global losses of SOC stocks, mainly due to the conversion of forests to cultivated lands.

### 6.3. Relative Permanence of Soil Properties and Revisit Time for Soil Monitoring

In Section 2, we described the relative permanencies of soil properties. One question is how these relative permanencies relate to current and future satellite revisit times. Indeed, it is a great advance that satellite revisit times are becoming shorter, especially with some of the commercially available data products with multiple weekly flybys.

Some applications might expect us to be able to deliver soil information corresponding to this time span. The challenge is the number of cloud-free days due to weather conditions, especially in the northern or mountainous regions of France. Even when there are no clouds, we may be confronted with shadow effects, and the topographic image corrections may not be accurate enough to monitor mountainous regions.

Another challenge is dealing with the observed spatial and temporal heterogeneity that is inconsistent with our understanding of the relative permanence and natural variability of soil properties. Finally, how do we translate this into effective sampling designs for soil monitoring? At field or farm-scale levels, UAV imagery helps design more efficient field sampling designs for monitoring, especially for SOC. It can also increase the density of observations in space and time and help to select the relevant soil signals and filter/correct

some perturbing factors. One challenge is to combine detailed surveys and RS products (from proximal sensing to UAV, airborne, and satellite data) in order to better calibrate the models obtained by hyperspectral and high-resolution satellite sensors and better design and optimize field sampling.

A final challenge is to make a clear distinction between what the changes in carbon storage and the changes in carbon sequestration are [179,215,260]. A promising way, at least for topsoil, could be to relate soil spectra to pools of SOC with different residence times. Several studies have shown the potential of laboratory Vis–NIR and MIR spectroscopy for an efficient estimation of SOC fractions, SOC monitoring, and modeling (e.g., [338–340]). To our knowledge, the feasibility of upscaling this kind of relationship to RS data needs to be assessed. This may increase the usefulness of RS to map and monitor SOC pools.

## 7. Main Progresses, Perspectives, and Prospects

### 7.1. The Increasing Availability of Remote Sensors and of Their Spatial, Spectral, and Temporal Resolution over Time

Taking the first Landsat satellite (1972) as a starting point, the last fifty years have been characterized by the launch of an increasing number of Earth observation satellites with different spatial coverages and resolutions, spectral bands, and revisiting times. Meanwhile, a large number of airborne spectral sensors have been tested on smaller spatial coverages in order to explore or simulate the potential of new sensors, to obtain faster images and shorten revisit times. These technological advances have improved the DSM in several ways:

The increase in spectral range and spectral band resolution has led to a drastic increase in the number of soil properties that can be predicted using RS (e.g., [43,107,341–345]).

The increase in spatial resolution allows the mapping of increasingly fine spatial distributions of soil properties and their controlling factors (e.g., [325,343,346]).

Shorter revisit periods allow for the better detection of changes in soil properties over shorter time periods and better capture of soil management effects (e.g., [347–350]).

Increasing the number of RS products over time allows both the design of composite products and a shift from static mapping to monitoring certain changes (e.g., [128,326,351]).

Merging data from RS products generally provides better predictions than using a single RS product (e.g., using a time series to increase both the prediction accuracy and map coverage [352], using synergistic information to retrieve soil information [353] or fusing products to increase both spatial and temporal resolution (e.g., [354–357])).

Several missions with high signal-to-noise ratios, high spatial resolution, but limited coverage per day have been launched recently: the Italian PRISMA (PRecursore Iper-Spettrale della Missione Applicativa, launch 22 March 2019, 30 m; [358,359]), the German EnMAP (Environmental Mapping and Analysis Program, launch 1 April 2022, 30 m, [360]), and the Japanese HISUI (Hyperspectral Imager Suite, launch 5 December 2019, 30 m; [361]). The Italian–Israeli SHALOM (Spaceborne Hyperspectral Applicative Land and Ocean Mission, launch 2024, 10 m [362]) is also expected to be launched soon. In addition, some global mapping missions are planned or under study for the coming years, with variable spatial coverage and different ground sampling distances, such as the former HypIRI mission [363,364] and the Sentinel-10/CHIME (Copernicus Hyperspectral Imaging Mission for the Environment) satellite proposed as an ESA candidate mission [365]. This wide range of satellites will represent a major step toward multi-resolution and multi-precisions soil mapping. Virtual satellite constellations (LANDSAT/S2, PLANET, EarthDaily . . . ) are promising tools for the future. One of the challenges is to harmonize the data because the sensors, acquisition conditions, and even the processing chains are different.

### 7.2. The Increasing Importance of RS Data in DSM

The trends we have observed and the future of RS in DSM can be schematically divided into the following two categories:

1. The use of RS products as surrogates for in situ measurements.
2. The incorporation of RS products as covariates for DSM.

In this section, we summarize the main conclusions that can be drawn from this review.

#### 7.2.1. Use of RS Products as Surrogates for In Situ Measurements

As developed in Section 3.4., and already highlighted by Lagacherie and Gomez [240], in some cases, “the estimations of soil properties at each pixel of a hyperspectral image is assumed to be precise enough to be considered as a measurement of a soil property and to be used as such for feeding DSM models”. The huge advantage of these situations is that the spatial sampling is much denser than what is usually available for the soil data to train DMS models. A better coverage of spatial soil variability, especially short-scale variability, which is often not captured by existing soil data, can be expected.

Moreover, there are still large spatial gaps in the available soil information to run DSM models around the world [13]. Therefore, these myriad surrogates for in situ measurements pave the way for both filling gaps in learning data and revealing finer spatial structures. These surrogates have proven to be efficient for some soil properties in the case of airborne hyperspectral imagery (e.g., [124,126,132,240,282]). However, we need to consider that these surrogates have uncertainties, and that the relationships that enabled the estimation of these surrogates should not be applied outside of their domain of validity. This is a big challenge, as soil data are still missing in large parts of the world.

#### 7.2.2. Incorporation of RS Products as Covariates in DSM

We have seen that RS products can be used as covariates in DSM models (see Section 4.2). This is primarily because many RS products not only reflect soil surface properties, but can provide spatiotemporal information about two categories of information that can be used in DSM.

RS products can provide information on the controlling factors of soil formation and changes. This is particularly the case for vegetation indexes, which provide indirect information about SOC inputs to soils. Conversely, soil moisture and temperature products can provide indirect information on the mineralization rate of SOC. Land cover and changes in land cover are related to different soil outputs and inputs that can influence pH, C and N cycles, nutrients, and possible sources of contamination. Airborne gamma-ray spectroscopy can provide information on the soil depth, presence of peats, soil weathering, and the nature and mineralogy of the parent material, or help better map clay content and/or mineralogy. The high-resolution DEMs derived from RS are essential to capture the different scales of soil processes and soil erosion/redistribution in the landscape at different scales. They are also very useful information for water redistribution and thus water regimes.

One big challenge with the multiplication of RS imagery is to conduct the right selection of covariates to avoid overfitting and respect the parsimony and relevance principles in DSM. Several ways of selecting covariates have been proposed and cited in this review. We must keep in mind that among the criteria used for selecting covariates and/or aggregating them in synthetic ones, we should take into account not only parsimony and redundancy, but also their meanings in terms of soil science. Conversely, another big challenge of DSM and data-driven modeling is to use them as knowledge discovery tools that may reveal or help with the understanding of new soil processes at various scales. In other words, RS and DSM are not only tools that can extend the spatially statistical relationships established on a set of leaning variates; they should also be able to discover new soil processes.

Although still underutilized, information on soil management practices at the field level is probably one of the most promising covariates with the development of hyperspectral sensors with high spatial and temporal resolution.

**Author Contributions:** Conceptualization, A.C.R.-d.-F. and D.A.; methodology, A.C.R.-d.-F.; data curation, A.C.R.-d.-F.; writing—original draft preparation, A.C.R.-d.-F.; writing—review and editing, A.C.R.-d.-F., Q.C., N.B., S.C., C.G., S.J., G.M., V.L.M., D.U.-S., E.V., M.W., J.-P.W. and D.A.; visualization, A.C.R.-d.-F.; supervision, D.A. and E.V.; project administration, E.V.; funding acquisition, E.V. All authors have read and agreed to the published version of the manuscript.

**Funding:** This review was supported by the THEIA TOSCA of the CNES and the MELICERTES project (ANR-22-PEAE-0010) of the French National Research Agency (France2030 and national PEPR “agroécologie et numérique” programmes). This review was supported by the European Joint Programme Cofund on Agricultural Soil Management (EJP-SOIL grant number 862695) and was carried out in the framework of the STEROPES project of EJP-SOIL. Qianqian Chen has been awarded a scholarship grant (202206320054) by the Chinese Scholarship Council to pursue her studies in France as a PhD student. D. Urbina-Salazar has received the support of a PhD scholarship from both INRAE (Institut national de recherche pour l’agriculture, l’alimentation et l’environnement) and ADEME (Agence de la transition écologique).

**Data Availability Statement:** There is no data to share. This is a review paper.

**Acknowledgments:** A.C. Richer-de-Forges is the coordinator of the Centre d’Etudes Scientifiques Theia “Cartographie Numérique des Sols” supported by the CNES, France. E. Vaudour, C. Gomez, G. Martelet, S. Jacquemoud, and D. Arrouays are members of this Centre d’Etudes Scientifiques Theia “Cartographie Numérique des Sols”. Thanks are expressed to the authors who allowed some figures of their original articles to be reproduced and/or adapted in this article (see references in the legends of Figures 5–9), and to ISRIC-World Soil Information, Elsevier®.

**Conflicts of Interest:** The authors declare no conflict of interest.

## Abbreviations

AVIRIS	Airborne Visible/Infrared Imaging Spectrometer
AWC	Available Water Capacity
CES	Scientific Expertise Center
CHIME	Copernicus Hyperspectral Imaging Mission for the Environment
CLAPAS	CLAssement des PAysages et Segmentation
cLHS	conditionnal Latin Hypercube Sampling
CNES	Centre National d’Etudes Spatiales (French Space Agency)
CNS	Cartographie Numérique des Sols (=DSM)
COP21	21st Conference Of the Parties of UN Climate Change Conferences
DEM	Digital Elevation Model
DSA	Digital Soil Assessment
DSM	Digital Soil Mapping
EnMAP	Environmental Mapping and Analysis Program
ESA	European Space Agency
ETM+	Enhanced Thematic Mapper Plus
EU	European Union
GSD	Ground Sampling Distance
HISUI	Hyperspectral Imager SUIt
INRAE	Institut national de recherche pour l’agriculture, l’alimentation et l’environnement (France)
IPCC	Intergovernmental Panel on Climate Change
L-MEB	L-band Microwave Emission of the Biosphere
LST	Land Surface Temperature
MIR	Middle Infrared
MIRS	Middle Infrared Spectroscopy
MODIS	Moderate Resolution Imaging Spectroradiometer
MW	MicroWave
NDVI	Normalized Difference Vegetation Index
NIR	Near Infra-Red
PLSR	Partial Least Squares Regression
PRISMA	PRecursores IperSpettrale della Missione Applicativa
PTF	PedoTransfer Function
RMSH	Root Mean Surface Height
RS	Remote Sensing
RZSM	Root Zone Soil Moisture

SAR	Synthetic Aperture Radar
SHALOM	Spaceborne Hyperspectral Applicative Land and Ocean Mission
SM	Soil Moisture
SMOS	Soil Moisture and Ocean Salinity
SOC	Soil Organic Carbon
SOM	Soil Organic Matter
SPOT	Système Probatoire d'Observation de la Terre/Satellite Pour l'Observation de la Terre
SRTM	Shuttle Radar Topographic Mission
TIR	Thermal Infra-Red
TSAVI	Transformed Soil-Adjusted Vegetation Index
UAV	Unmanned Aerial Vehicle
UN	United Nations
USGS	United States Geological Survey
Vis-NIR	Visible and Near Infra-Red
VOD	Vegetation Optical Depth

## References

- McBratney, A.; Field, D.J.; Koch, A. The Dimensions of Soil Security. *Geoderma* **2014**, *213*, 203–213. [CrossRef]
- Amundson, R.; Berhe, A.A.; Hopmans, J.W.; Olson, C.; Sztein, A.E.; Sparks, D.L. Soil and Human Security in the 21st Century. *Science* **2015**, *348*, 1261071. [CrossRef] [PubMed]
- FAO-ITPS. *Status of the World's Soil Resources (SWSR). Main Report. Technical Panel on Soils*; Food and Agriculture Organization of the United Nations and Intergovernmental: Rome, Italy, 2015; p. 94.
- Montanarella, L.; Pennock, D.J.; McKenzie, N.; Badraoui, M.; Chude, V.; Baptista, I.; Mamo, T.; Yemefack, M.; Singh Aulakh, M.; Yagi, K.; et al. World's Soils Are under Threat. *SOIL* **2016**, *2*, 79–82. [CrossRef]
- Bouma, J.; Montanarella, L. Facing Policy Challenges with Inter- and Transdisciplinary Soil Research Focused on the UN Sustainable Development Goals. *SOIL* **2016**, *2*, 135–145. [CrossRef]
- Keesstra, S.D.; Bouma, J.; Wallinga, J.; Titttonell, P.; Smith, P.; Cerdà, A.; Montanarella, L.; Quinton, J.N.; Pachepsky, Y.; van der Putten, W.H.; et al. The Significance of Soils and Soil Science towards Realization of the United Nations Sustainable Development Goals. *SOIL* **2016**, *2*, 111–128. [CrossRef]
- Bouma, J. How to Communicate Soil Expertise More Effectively in the Information Age When Aiming at the UN Sustainable Development Goals. *Soil Use Manag.* **2019**, *35*, 32–38. [CrossRef]
- Bonfante, A.; Basile, A.; Bouma, J. Targeting the Soil Quality and Soil Health Concepts When Aiming for the United Nations Sustainable Development Goals and the EU Green Deal. *SOIL* **2020**, *6*, 453–466. [CrossRef]
- Panagos, P.; Montanarella, L. Soil Thematic Strategy: An Important Contribution to Policy Support, Research, Data Development and Raising the Awareness. *Curr. Opin. Environ. Sci. Health* **2018**, *5*, 38–41. [CrossRef]
- European Commission. EU Soil Strategy for 2030, Section 3.2.2. 2022. Available online: <https://eur-lex.europa.eu/legal-content/EN/TXT/?uri=CELEX%3A52021DC0699> (accessed on 29 May 2023).
- McBratney, A.B.; Mendonça Santos, M.L.; Minasny, B. On Digital Soil Mapping. *Geoderma* **2003**, *117*, 3–52. [CrossRef]
- Minasny, B.; McBratney, A.B. Digital Soil Mapping: A Brief History and Some Lessons. *Geoderma* **2016**, *264*, 301–311. [CrossRef]
- Arrouays, D.; Lagacherie, P.; Hartemink, A.E. Digital Soil Mapping across the Globe. *Geoderma Reg.* **2017**, *9*, 1–4. [CrossRef]
- Lagacherie, P.; McBratney, A.B.; Voltz, M. (Eds.) *Digital Soil Mapping: An Introductory Perspective*, 1st ed.; Developments in Soil Science; Elsevier: Amsterdam, The Netherlands, 2006; ISBN 978-0-444-52958-9.
- Jenny, H. *Factors of Soil Formation: A System of Quantitative Pedology*; McGraw-Hill: New York, NY, USA, 1941; ISBN 978-0-486-68128-3.
- Grunwald, S. Multi-Criteria Characterization of Recent Digital Soil Mapping and Modeling Approaches. *Geoderma* **2009**, *152*, 195–207. [CrossRef]
- Minasny, B.; McBratney, A.B. Methodologies for Global Soil Mapping. In *Digital Soil Mapping. Bridging Research, Environmental Application and Operation*; Boettinger, J.L., Howell, D.W., Moore, A.C., Hartemink, A.E., Kienast-Brown, S., Eds.; Springer: Dordrecht, The Netherlands, 2010.
- Zhang, G.; Liu, F.; Song, X. Recent Progress and Future Prospect of Digital Soil Mapping: A Review. *J. Integr. Agric.* **2017**, *16*, 2871–2885. [CrossRef]
- Wadoux, A.M.J.-C.; Minasny, B.; McBratney, A.B. Machine Learning for Digital Soil Mapping: Applications, Challenges and Suggested Solutions. *Earth-Sci. Rev.* **2020**, *210*, 103359. [CrossRef]
- Arrouays, D.; McBratney, A.; Bouma, J.; Libohova, Z.; Richer-de-Forges, A.C.; Morgan, C.L.S.; Roudier, P.; Poggio, L.; Mulder, V.L. Impressions of Digital Soil Maps: The Good, the Not so Good, and Making Them Ever Better. *Geoderma Reg.* **2020**, *20*, e00255. [CrossRef]
- Chen, S.; Arrouays, D.; Leatitia Mulder, V.; Poggio, L.; Minasny, B.; Roudier, P.; Libohova, Z.; Lagacherie, P.; Shi, Z.; Hannam, J.; et al. Digital Mapping of GlobalSoilMap Soil Properties at a Broad Scale: A Review. *Geoderma* **2022**, *409*, 115567. [CrossRef]



22. Dvorakova, K.; Heiden, U.; Pepers, K.; Staats, G.; van Os, G.; van Wesemael, B. Improving Soil Organic Carbon Predictions from a Sentinel-2 Soil Composite by Assessing Surface Conditions and Uncertainties. *Geoderma* **2023**, *429*, 116128. [[CrossRef](#)]
23. Zhang, C.; Valente, J.; Kooistra, L.; Guo, L.; Wang, W. Orchard Management with Small Unmanned Aerial Vehicles: A Survey of Sensing and Analysis Approaches. *Precis. Agric.* **2021**, *22*, 2007–2052. [[CrossRef](#)]
24. Ustin, S.L.; Middleton, E.M. Current and Near-Term Advances in Earth Observation for Ecological Applications. *Ecol. Process.* **2021**, *10*, 1. [[CrossRef](#)]
25. Heiden, U.; d'Angelo, P.; Schwind, P.; Karlsrufer, P.; Müller, R.; Zepp, S.; Wiesmeier, M.; Reinartz, P. Soil Reflectance Composites—Improved Thresholding and Performance Evaluation. *Remote Sens.* **2022**, *14*, 4526. [[CrossRef](#)]
26. Segalen, P. *L'interprétation Des Photographies Aériennes En Vue de La Cartographie Pédologique*; IRCAM: Yaoundé, Cameroon, 1961; p. 20.
27. Maignien, R. La Photo-Interprétation En Pédologie. *Cah. ORSTOM* **1963**, *3*, 8–16.
28. Dupuis, P.; Callot, M. De l'utilisation de La Photographie Aérienne En Cartographie Pédologique. *Bull. A.F.E.S. Paris* **1965**, *12*, 424–446.
29. Pouquet, J. *Les Sciences de La Terre à l'heure Des Satellites*; Presses Universitaires de France: Paris, France, 1971.
30. Verger, F. L'observation de la terre par les satellites, Presses universitaires de France, coll. «Que sais-je?», n 1989, 128 p. *Géographie Phys. Quat.* **1982**, *36*, 128. [[CrossRef](#)]
31. Girard, M.C.; Girard, C.M. *Applications de La Télédétection à l'étude de La Biosphère*; Masson: Paris, France, 1974.
32. Girard, M.C.; Girard, C.M. *Télédétection Appliquée: Zones Tempérées et Intertropicales*; Collection Sciences Agronomiques; Masson: Paris, France, 1989; ISBN 978-2-225-81202-6.
33. Girard, M.C.; Girard, C.M. *Processing of Remote Sensing Data*; Oxford & IBH Publishing, Co.: New Delhi, India, 2003.
34. Scanvic, J.-Y. *Utilisation de La Télédétection Dans Les Sciences de La Terre*; Manuels et Méthodes; BRGM: Orléans, France, 1983; ISBN 978-2-7159-0021-9.
35. Cervelle, B.; Malézieux, J.-M.; Caye, R. Expression quantitative de la couleur, liée à la réflectance diffuse, de quelques roches et minéraux. *Bull. Société Française Minéralogie Cristallogr.* **1977**, *100*, 185–191. [[CrossRef](#)]
36. Cervelle, B.; Lévy, C.; Henry, N.-F.-M.; Shadlun, T.N. Développement récents dans la mesure au microscope des réflectances spectrales des minéraux opaques. *Bull. Minéralogie* **1978**, *101*, 234–244. [[CrossRef](#)]
37. Ducasse, E.; Adeline, K.; Briottet, X.; Hohmann, A.; Bourguignon, A.; Grandjean, G. Montmorillonite Estimation in Clay-Quartz-Calcite Samples from Laboratory SWIR Imaging Spectroscopy: A Comparative Study of Spectral Preprocessings and Unmixing Methods. *Remote Sens.* **2020**, *12*, 1723. [[CrossRef](#)]
38. de Cailleux, A. Mesure simple de l'albédo en géographie. *Ann. Géographie* **1974**, *83*, 569–585. [[CrossRef](#)]
39. Girard, M.-C. Emploi de La Télédétection Pour l'étude de l'humidité Des Sols. *Houille Blanche* **1978**, *64*, 533–539. [[CrossRef](#)]
40. Courault, D. A Study on the Degradation of the Land Surface by Remote Sensing. Spectral, Spatial and Temporal Analysis. Ph.D. Thesis, University of Paris, Paris, France, 1989.
41. Mougénot, B. Effets Des Sels Sur La Réflectance et Télédétection Des Sols Salés. *Cah. ORSTOM* **1993**, *28*, 45–54.
42. Chanzy, A. Basic Soil Surface Characteristics Derived from Active Microwave Remote Sensing. *Remote Sens. Rev.* **1993**, *7*, 303–319. [[CrossRef](#)]
43. Lagacherie, P.; Baret, F.; Feret, J.; Netto, J.; Robbez-Masson, J. Estimation of Soil Clay and Calcium Carbonate Using Laboratory, Field and Airborne Hyperspectral Measurements. *Remote Sens. Environ.* **2008**, *112*, 825–835. [[CrossRef](#)]
44. Liu, W.; Baret, F.; Gu, X.; Zhang, B.; Tong, Q.; Zheng, L. Evaluation of Methods for Soil Surface Moisture Estimation from Reflectance Data. *Int. J. Remote Sens.* **2003**, *24*, 2069–2083. [[CrossRef](#)]
45. Liu, W.; Baret, F.; Gu, X.; Tong, Q.; Zheng, L.; Zhang, B. Relating Soil Surface Moisture to Reflectance. *Remote Sens. Environ.* **2002**, *81*, 238–246.
46. Escadafal, R.; Girard, M.-C.; Courault, D. Modelling the Relationships between Munsell Soil Color and Soil Spectral Properties. *Int. Agrophysics* **1988**, *4*, 249–261.
47. Wassenaar, T.; Andrieux, P.; Baret, F.; Robbez-Masson, J. Soil Surface Infiltration Capacity Classification Based on the Bi-Directional Reflectance Distribution Function Sampled by Aerial Photographs. The Case of Vineyards in a Mediterranean Area. *CATENA* **2005**, *62*, 94–110. [[CrossRef](#)]
48. Mougénot, B.; Pouget, M.; Epema, G.F. Remote Sensing of Salt Affected Soils. *Remote Sens. Rev.* **1993**, *7*, 241–259. [[CrossRef](#)]
49. Escadafal, R. Remote Sensing of Arid Soil Surface Color with Landsat Thematic Mapper. *Adv. Space Res.* **1989**, *9*, 159–163. [[CrossRef](#)]
50. Escadafal, R.; Huete, A. Etude des propriétés spectrales des sols arides appliquée à l'amélioration des indices de végétation obtenus par télédétection. *Comptes Rendus L'académie Sci.* **1991**, *312*, 1385–1391.
51. Mathieu, R.; Pouget, M.; Cervelle, B.; Escadafal, R. Relationships between Satellite-Based Radiometric Indices Simulated Using Laboratory Reflectance Data and Typic Soil Color of an Arid Environment. *Remote Sens. Environ.* **1998**, *66*, 17–28. [[CrossRef](#)]
52. Baret, F.; Guyot, G. Potentials and Limits of Vegetation Indexes for LAI and APAR Assessment. *Remote Sens. Environ.* **1991**, *35*, 161–173. [[CrossRef](#)]
53. Baret, F.; Jacquemoud, S.; Hanocq, J.F. About the Soil Line Concept in Remote Sensing. *Adv. Space Res.* **1993**, *13*, 281–284. [[CrossRef](#)]

54. Cierniewski, J.; Baret, F.; Verbrugge, M.; Hanocq, J.; Jacquemoud, S. Geometrical Modelling of Soil Bidirectional Reflectance Incorporating Specular Effects. *Int. J. Remote Sens.* **1996**, *17*, 3691–3704. [[CrossRef](#)]
55. Cierniewski, J.; Verbrugge, M. Influence of Soil Surface Roughness on Soil Bidirectional Reflectance. *Int. J. Remote Sens.* **1997**, *18*, 1277–1288. [[CrossRef](#)]
56. Jacquemoud, S.; Baret, F.; Hanocq, J.F. Modeling Spectral and Bidirectional Soil Reflectance. *Remote Sens. Environ.* **1992**, *41*, 123–132. [[CrossRef](#)]
57. Bablet, A.; Vu, P.; Jacquemoud, S.; Viallefont-Robinet, F.; Fabre, S.; Briottet, X.; Sadeghi, M.; Whiting, M.; Baret, F.; Tian, J. MARMIT: A Multilayer Radiative Transfer Model of Soil Reflectance to Estimate Surface Soil Moisture Content in the Solar Domain (400–2500 nm). *Remote Sens. Environ.* **2018**, *217*, 1–17. [[CrossRef](#)]
58. Dupiau, A.; Jacquemoud, S.; Briottet, X.; Fabre, S.; Viallefont-Robinet, F.; Philpot, W.; Di Biagio, C.; Hebert, M.; Formenti, P. MARMIT-2: An Improved Version of the MARMIT Model to Predict Soil Reflectance as a Function of Surface Water Content in the Solar Domain. *Remote Sens. Environ.* **2022**, *272*, 112951. [[CrossRef](#)]
59. Lesaignoux, A.; Fabre, S.; Briottet, X.; Olioso, A. Soil Moisture Impact on Lab Measured Reflectance of Bare Soils in the Optical Domain [0.4–15  $\mu$ m]. In Proceedings of the 2009 IEEE International Geoscience and Remote Sensing Symposium, Cape Town, South Africa, 12–17 July 2009; p. 1824.
60. Verbrugge, M.; Cierniewski, J. Influence and Modelling of View Angles and Microrelief on Surface Temperature Measurements of Bare Agricultural Soils. *ISPRS J. Photogramm. Remote Sens.* **1998**, *53*, 166–173. [[CrossRef](#)]
61. Girard, M.C. Apport de l'interprétation Visuelle Des Images Satellitaires Pour l'analyse Spatiale Des Sols. Un Exemple Dans La Région de Lodève. *Etude Gest. Sols* **1995**, *2*, 7–24.
62. Girard, M.-C.; Rogala, J.-P. Analyse de l'environnement par traitement informatique des données Landsat. Un exemple: L'humidité des sols. *Intern. Arch. Photogram.* **1980**, *XXIII*, 335–344.
63. Escadafal, R.; Mtimet, A. Apport de La Télédétection Spatiale à La Cartographie Des Sols de La Région de Médénine (Sud-Tunisien); Etudes Spéciales—Division des Sols; Direction des Sols, DRES: Tunis, Tunisia, 1981; p. 40.
64. Arrouays, D.; Guyon, D.; Riom, J. Différenciation Par l'humidité et La Matière Organique de Deux Sols Sableux à Partir de Données Radiométriques et Photographiques. *Colloq. INRA* **1984**, *23*, 81–89.
65. King, C. Etude Des Sols et Des Formations Superficielles Par Télédétection: Approche de Leurs Caractéristiques Spectrales Spatiales et Temporelles Dans Le Visible et Le Proche Infra-Rouge. Ph.D. Thesis, INA-PG, Paris, France, 1985.
66. Dosso, M. Analyse Structurale d'une Unité de Modelé Latéritique Comme Référence Pour La Recherche d'informations Pédologiques d'ordre Structural Contenus Dans Les Images de Télédétection Correspondantes; ORSTOM: Douala, Cameroun, 1986; pp. 211–220.
67. Dosso, M.; Seyler, F.; Bocquier, G.; Ruellan, A. Analysis of Soil Organization; Regional Mapping Using Remote Sensing; Examples in Brittany (France) and French Guiana. XII AISS Congress; Hamburg, Germany, 13–20 August 1986; pp. 1099–1100.
68. Arrouays, D. Un Exemple D'utilisation de La Télédétection Pour La Réalisation D'une Carte Des Sols à Moyenne Échelle. In Proceedings of the Actes du Séminaire INRA Projet Télédétection, Monetier-les-Bains, Hautes-Alpes, France, 12–16 January 1987; pp. 275–280.
69. Courault, D.; Girard, M.C. Analyse Des Hétérogénéités Intraparcellaires Des Sols Par Télédétection. *Sci. Sol.* **1988**, *26*, 1–12.
70. El-Hady, A.M.A.; Rognon, P.; Escadafal, R.; Pouget, M. Contribution of Landsat Data (MSS) to Soil Survey: Application to the Soil of Southwestern Sinai (Egypt). *Int. J. Remote Sens.* **1991**, *12*, 1053–1061. [[CrossRef](#)]
71. Rudant, J.P.; Derotn, J.P.; Polidori, L. Multi-Resolution Analysis of Radar Images and Its Application to Lithological and Structural Mapping; Larzac (Southern France) Test Site. *Int. J. Remote Sens.* **1994**, *15*, 2451–2468. [[CrossRef](#)]
72. Vaudour, E.; Girard, M.-C.; Bremond, L.-M.; Lurton, L. Spatial terroir characterization and grape composition in the Southern Côtes-du-Rhône vineyard (Nyons-Valreas Basin). *OENO One* **1998**, *32*, 169. [[CrossRef](#)]
73. Kouame, J.L.; Classeau, N.; Rudant, J.-P.; Trebossen, H. Evaluation of the Potential of Radar ENVISAT Data for the Updating of Numerical Thematic Maps on the Coastal Fringe of French Guyana. In Proceedings of the IGARSS 2003, IEEE International Geoscience and Remote Sensing Symposium, Toulouse, France, 21–25 July 2003; pp. 3718–3720.
74. Vaudour, E. *Les Terroirs Viticoles: Définitions, Caractérisation et Protection*; Dunod: Paris, France, 2003; ISBN 978-2-10-006454-0.
75. Vaudour, E. Remote Sensing of Red Mediterranean Soils: A Case Study in the Viticultural Southern Rhone Valley Using SPOT Satellite Imagery. *Geocarto Int.* **2008**, *23*, 197–216. [[CrossRef](#)]
76. Bou Kheir, R.; Girard, M.; Khawlie, M. Use of the OASIS structural classification system for mapping the landscape unites in a representative region of Lebanon. *Can. J. Remote Sens.* **2004**, *30*, 617–630. [[CrossRef](#)]
77. Vaudour, E.; Carey, V.A.; Gilliot, J.M. Digital Zoning of South African Viticultural Terroirs Using Bootstrapped Decision Trees on Morphometric Data and Multitemporal SPOT Images. *Remote Sens. Environ.* **2010**, *114*, 2940–2950. [[CrossRef](#)]
78. Lesaignoux, A.; Fabre, S.; Briottet, X. Influence of Soil Moisture Content on Spectral Reflectance of Bare Soils in the 0.4–14  $\mu$ m Domain. *Int. J. Remote Sens.* **2013**, *34*, 2268–2285. [[CrossRef](#)]
79. Fabre, S.; Briottet, X.; Lesaignoux, A. Estimation of Soil Moisture Content from the Spectral Reflectance of Bare Soils in the 0.4–2.5  $\mu$ m Domain. *Sensors* **2015**, *15*, 3262–3281. [[CrossRef](#)]
80. Escadafal, R.; Girard, M.-C.; Courault, D. Munsell Soil Color and Soil Reflectance in the Visible Spectral Bands of Landsat MSS and TM Data. *Remote Sens. Environ.* **1989**, *27*, 37–46. [[CrossRef](#)]
81. Bernard, R.; Martin, P.; Thony, J.-L.; Vauclin, M.; Vidal-Madjar, D. C-Band Radar for Determining Surface Soil Moisture. *Remote Sens. Environ.* **1982**, *12*, 189–200. [[CrossRef](#)]

82. Brun, C.; Vidal-Madjar, D.; Gascuel-Oudou, C.; Merot, P.; Duchesne, J.; Nicolas, H. Locating Saturated Areas over a Watershed by Using Helicopter-Borne C-Band Scatterometer. *Water Resour. Res.* **1987**, *26*, 945–955.
83. Muller, E.; Decamps, H. Modeling Soil Moisture-Reflectance. *Remote Sens. Environ.* **2001**, *76*, 173–180. [[CrossRef](#)]
84. Pellarin, T.; Wigneron, J.; Calvet, J.; Berger, M.; Douville, H.; Ferrazzoli, P.; Kerr, Y.; Lopez-Baeza, E.; Pulliainen, J.; Simmonds, L.; et al. Two-Year Global Simulation of L-Band Brightness Temperatures over Land. *IEEE Trans. Geosci. Remote Sens.* **2003**, *41*, 2135–2139. [[CrossRef](#)]
85. Parde, M.; Wigneron, J.-P.; Chanzy, A.; Waldteufel, P.; Schmidl, S.; Skou, N. Soil Moisture Retrieval from L-Band Measurements over a Variety of Agricultural Crops. In Proceedings of the IGARSS 2003, IEEE International Geoscience and Remote Sensing Symposium, Toulouse, France, 21–25 July 2003; pp. 914–916.
86. El Hajj, M.; Baghdadi, N.; Zribi, M.; Bazzi, H. Synergic Use of Sentinel-1 and Sentinel-2 Images for Operational Soil Moisture Mapping at High Spatial Resolution over Agricultural Areas. *Remote Sens.* **2017**, *9*, 1292. [[CrossRef](#)]
87. Boissard, P.; Pointel, J.-G.; Renaux, B.; Begon, J.-C. Zonage et Quantification de La Stabilité Structurale de Sols Cultivés Basés Sur Des Données Du Satellite Landsat-TM, Application Au Cas d'une Parcelle d'orge En Beauce. *Comptes Rendus L'académie Sci. Paris Série II Pédologie* **1989**, *309*, 145–152.
88. de Jong, S.M. Derivation of Vegetative Variables from a Landsat Tm Image for Modelling Soil Erosion. *Earth Surf. Process. Landf.* **1994**, *19*, 165–178. [[CrossRef](#)]
89. Arrouays, D.; King, C.; Vion, I.; Le Bissonnais, Y. Detection of Soil Crusting Risks Related to Low Soil Organic Carbon Contents by Using Discriminant Analysis on Thematic Mapper Data. *Geocarto Int.* **1996**, *11*, 11–16. [[CrossRef](#)]
90. Biard, F.; Baret, F. CRIM: Crop Residue Index to Monitor Erosion. In Proceedings of the Seventh International Symposium on Physical Measurements and Signatures in Remote Sensing, Courchevel, France, 7–11 April 1997; Guyot, G., Phulpin, T., Eds.; Routledge & CRC Press Balkema: Rotterdam, The Netherlands; Volume 2, pp. 421–429.
91. de Jong, S.M.; Paracchini, M.L.; Bertolo, F.; Folving, S.; Megier, J.; de Roo, A.P.J. Regional Assessment of Soil Erosion Using the Distributed Model SEMMED and Remotely Sensed Data. *CATENA* **1999**, *37*, 291–308. [[CrossRef](#)]
92. Baghdadi, N.; King, C.; Bourguignon, A.; Remond, A. Potential of ERS and RADARSAT Data for Surface Roughness Monitoring over Bare Agricultural Fields Affected by Excessive Runoff. In Proceedings of the IGARSS 2000, IEEE 2000 International Geoscience and Remote Sensing Symposium, Taking the Pulse of the Planet: The Role of Remote Sensing in Managing the Environment, Honolulu, HI, USA, 24–28 July 2000; pp. 1907–1909.
93. Baghdadi, N.; King, C.; Bourguignon, A.; Remond, A. Potential of ERS and Radarsat Data for Surface Roughness Monitoring over Bare Agricultural Fields: Application to Catchments in Northern France. *Int. J. Remote Sens.* **2002**, *23*, 3427–3442. [[CrossRef](#)]
94. Coulombe-Simoneau, J.; Hardy, S.; Baghdadi, N.; King, C.; Bonn, F.; Le Bissonnais, Y. Radarsat Based Monitoring of Soil Roughness over an Agricultural Area Affected by Excessive Runoff. In Proceedings of the International Symposium on Remote Sensing and Hydrology 2000, Santa Fé, NM, USA, 2–8 April 2000; pp. 362–364.
95. Gay, M.; Cheret, V.; Denux, J. Remote sensed data contribution to erosion risks identification. *Houille Blanche-Rev. Int. L'eau* **2002**, *88*, 81–86. [[CrossRef](#)]
96. Houet, T.; Hubert-Moy, L.; Mercier, G.; Gouery, P. Estimation and Monitoring of Bare Soil/Vegetation Ratio with SPOT Vegetation and HRVIR. In Proceedings of the Centre National de la Recherche Scientifique (CNRS), Toulouse, France, 21–25 July 2003; pp. 3248–3250.
97. Souchère, V.; Cerdan, O.; Dubreuil, N.; Le Bissonnais, Y.; King, C. Modelling the Impact of Agri-Environmental Scenarios on Runoff in a Cultivated Catchment (Normandy, France). *CATENA* **2005**, *61*, 229–240. [[CrossRef](#)]
98. Aubert, M.; Baghdadi, N.; Zribi, M.; Douaoui, A.; Loumagne, C.; Baup, F.; El Hajj, M.; Garrigues, S. Analysis of TerraSAR-X Data Sensitivity to Bare Soil Moisture, Roughness, Composition and Soil Crust. *Remote Sens. Environ.* **2011**, *115*, 1801–1810. [[CrossRef](#)]
99. Mougenot, B.; Zante, P.; Montoroi, J.-P. Détection et Évolution Saisonnière Des Sols Salés et Acidifiés Du Domaine Fluvio-Marin de Basse Casamance Au Sénégal, Par Imagerie Satellitari. In *Apports de la Télédétection à la Lutte Contre la Sécheresse*; Lafrance, P., Dubois, J.M., Eds.; J. Libbey editions: Paris, France, 1990.
100. Mougenot, B.; Cailleau, D. Identification par télédétection des sols dégradés d'un domaine sahélien au Niger. In *Surveillance des Sols Dans L'environnement Par Télédétection et Systèmes D'information Géographiques: Actes du Symposium International AISS, . . . , Ouagadougou, Burkina Faso, Du 6 Au 10 Février 1995 = Monitoring Soils in the Environment with Remote Sensing and Gis: Proceedings of the ISSS International Symposium, . . . , Ouagadougou, Burkina Faso, 6–10 February 1995*; Escadafal, R., Mulders, M.A., Thiombiano, L., Association Internationale de la Science du Sol, Eds.; Collection Colloques et Séminaires; ORSTOM: Paris, France, 1996; ISBN 978-2-7099-1331-7.
101. Moussa, I.; Walter, C.; Michot, D.; Adam Boukary, I.; Nicolas, H.; Pichelin, P.; Guéro, Y. Soil Salinity Assessment in Irrigated Paddy Fields of the Niger Valley Using a Four-Year Time Series of Sentinel-2 Satellite Images. *Remote Sens.* **2020**, *12*, 3399. [[CrossRef](#)]
102. Ouerghemmi, W.; Gomez, C.; Naceur, S.; Lagacherie, P. Applying Blind Source Separation on Hyperspectral Data for Clay Content Estimation over Partially Vegetated Surfaces. *Geoderma* **2011**, *163*, 227–237. [[CrossRef](#)]
103. Qi, J.; Chehbouni, A.; Huete, A.; Kerr, Y.; Sorooshian, S. A Modified Soil Adjusted Vegetation Index. *Remote Sens. Environ.* **1994**, *48*, 119–126. [[CrossRef](#)]
104. Rondeaux, G.; Steven, M.; Baret, F. Optimization of Soil-Adjusted Vegetation Indices. *Remote Sens. Environ.* **1996**, *55*, 95–107. [[CrossRef](#)]

105. Vaudour, E.; Girard, M. Pédologie. Chapitre 23; In *Traitement des Images de Télédétection*; Girard, M., Girard, C., Eds.; Dunod: Paris, France, 2010.
106. Ben-Dor, E.; Irons, J.A.; Epema, A. Soil Spectroscopy. In *Manual of Remote Sensing*; Rencz, A., Ed.; John Wiley & Sons: New York, NY, USA, 1999; pp. 111–188.
107. Ben-Dor, E.; Chabrillat, S.; Demattê, J.A.M.; Taylor, G.R.; Hill, J.; Whiting, M.L.; Sommer, S. Using Imaging Spectroscopy to Study Soil Properties. *Remote Sens. Environ.* **2009**, *113*, S38–S55. [[CrossRef](#)]
108. Ben-Dor, E. Quantitative Remote Sensing of Soil Properties. *Adv. Agron.* **2002**, *75*, 173–243.
109. Mulder, V.L.; de Bruin, S.; Schaepman, M.E.; Mayr, T.R. The Use of Remote Sensing in Soil and Terrain Mapping—A Review. *Geoderma* **2011**, *162*, 1–19. [[CrossRef](#)]
110. Demattê, J.A.M.; Morgan, C.; Chabrillat, S.; Rizzo, R.; Franceschini, M.H.D.; Terra, F.D.S.; Vasques, G.M.; Wetterlind, J. Spectral Sensing from Ground to Space in Soil Science: State of the Art, Applications, Potential, and Perspectives. In *Land Resources Monitoring, Modeling, and Mapping with Remote Sensing*; CRC Press-Taylor & Francis Group: Boca Raton, FL, USA, 2016.
111. Chabrillat, S.; Ben-Dor, E.; Cierniewski, J.; Gomez, C.; Schmid, T.; van Wesemael, B. Imaging Spectroscopy for Soil Mapping and Monitoring. *Surv. Geophys.* **2019**, *40*, 361–399. [[CrossRef](#)]
112. Tziolas, N.; Tsakiridis, N.; Chabrillat, S.; Demattê, J.A.M.; Ben-Dor, E.; Gholizadeh, A.; Zalidis, G.; van Wesemael, B. Earth Observation Data-Driven Cropland Soil Monitoring: A Review. *Remote Sens.* **2021**, *13*, 4439. [[CrossRef](#)]
113. Richer-de-Forges, A.C.; Lagacherie, P.; Arrouays, D.; Bialkowski, A.; Bourennane, H.; Briottet, X.; Fouad, Y.; Gomez, C.; Jacquemoud, S.; Lemerrier, B.; et al. The Theia “Digital Soil Mapping” Scientific Expertise Centre of France. *Pedometron* **2022**, *46*, 4–8.
114. Richer-de-Forges, A.C.; Lagacherie, P.; Arrouays, D.; Bialkowski, A.; Bourennane, H.; Briottet, X.; Bustillo, V.; Fouad, Y.; Gomez, C.; Jacquemoud, S.; et al. The Theia “Digital Soil Mapping” Scientific Expertise Centre of France. In *Proceedings of the Soil Mapping for a Sustainable Future, 2nd Joint Workshop of the IUSS Working Groups Digital Soil Mapping and Global Soil Map, Orléans, France, 7–9 February 2023*.
115. Droogers, P.; Bouma, J. Soil Survey Input in Exploratory Modeling of Sustainable Soil Management Practices. *Soil Sci. Soc. Am. J.* **1997**, *61*, 1704–1710. [[CrossRef](#)]
116. IUSS Working Group. WRB World Reference Base for Soil Resources 2014, Update 2015. International Soil Classification System for Naming Soils and Creating Legends for Soil Maps. World Soil Resources Reports No. 106. FAO, Rome. 2015. Available online: <https://www.fao.org/3/i3794en/I3794en.pdf> (accessed on 29 May 2023).
117. Bouma, J.; Droogers, P. Comparing Different Methods for Estimating the Soil Moisture Supply Capacity of a Soil Series Subjected to Different Types of Management. *Geoderma* **1999**, *92*, 185–197. [[CrossRef](#)]
118. Sonneveld, M.P.W.; Bouma, J.; Veldkamp, A. Refining Soil Survey Information for a Dutch Soil Series Using Land Use History. *Soil Use Manag.* **2002**, *18*, 157–163. [[CrossRef](#)]
119. Stevenson, B.A.; McNeill, S.; Hewitt, A.E. Characterising Soil Quality Clusters in Relation to Land Use and Soil Order in New Zealand: An Application of the Phenoform Concept. *Geoderma* **2015**, *239–240*, 135–142. [[CrossRef](#)]
120. Rossiter, D.G.; Bouma, J. A New Look at Soil Phenoforms—Definition, Identification, Mapping. *Geoderma* **2018**, *314*, 113–121. [[CrossRef](#)]
121. Peng, J.; Albergel, C.; Balenzano, A.; Brocca, L.; Cartus, O.; Cosh, M.; Crow, W.; Dabrowska-Zielinska, K.; Dadson, S.; Davidson, M.; et al. A Roadmap for High-Resolution Satellite Soil Moisture Applications—Confronting Product Characteristics with User Requirements. *Remote Sens. Environ.* **2021**, *252*, 112162. [[CrossRef](#)]
122. Ward, K.J.; Chabrillat, S.; Brell, M.; Castaldi, F.; Spengler, D.; Foerster, S. Mapping Soil Organic Carbon for Airborne and Simulated EnMAP Imagery Using the LUCAS Soil Database and a Local PLSR. *Remote Sens.* **2020**, *12*, 3451. [[CrossRef](#)]
123. Vaudour, E.; Gomez, C.; Fouad, Y.; Lagacherie, P. Sentinel-2 Image Capacities to Predict Common Topsoil Properties of Temperate and Mediterranean Agroecosystems. *Remote Sens. Environ.* **2019**, *223*, 21–33. [[CrossRef](#)]
124. Gomez, C.; Lagacherie, P.; Bacha, S. Using an VNIR/SWIR Hyperspectral Image to Map Topsoil Properties over Bare Soil Surfaces in the Cap Bon Region (Tunisia). In *Digital Soil Assessments and Beyond*; Minasny, B., Malone, B.P., McBratney, A.B., Eds.; Springer: Berlin/Heidelberg, Germany, 2012; pp. 387–392.
125. Ivushkin, K.; Bartholomeus, H.; Bregt, A.K.; Pulatov, A.; Kempen, B.; de Sousa, L. Global Mapping of Soil Salinity Change. *Remote Sens. Environ.* **2019**, *231*, 111260. [[CrossRef](#)]
126. Gomez, C.; Lagacherie, P.; Coulouma, G. Regional Predictions of Eight Common Soil Properties and Their Spatial Structures from Hyperspectral Vis–NIR Data. *Geoderma* **2012**, *189–190*, 176–185. [[CrossRef](#)]
127. Gomez, C.; Gholizadeh, A.; Borůvka, L.; Lagacherie, P. Using Legacy Data for Correction of Soil Surface Clay Content Predicted from VNIR/SWIR Hyperspectral Airborne Images. *Geoderma* **2016**, *276*, 84–92. [[CrossRef](#)]
128. Vaudour, E.; Gomez, C.; Lagacherie, P.; Loiseau, T.; Baghdadi, N.; Urbina-Salazar, D.; Loubet, B.; Arrouays, D. Temporal Mosaicking Approaches of Sentinel-2 Images for Extending Topsoil Organic Carbon Content Mapping in Croplands. *Int. J. Appl. Earth Obs. Geoinf.* **2021**, *96*, 102277. [[CrossRef](#)]
129. Urbina-Salazar, D.; Vaudour, E.; Baghdadi, N.; Ceschia, E.; Richer-de-Forges, A.C.; Lehmann, S.; Arrouays, D. Using Sentinel-2 Images for Soil Organic Carbon Content Mapping in Croplands of Southwestern France. The Usefulness of Sentinel-1/2 Derived Moisture Maps and Mismatches between Sentinel Images and Sampling Dates. *Remote Sens.* **2021**, *13*, 5115. [[CrossRef](#)]

130. Gasmi, A.; Gomez, C.; Lagacherie, P.; Zouari, H. Surface Soil Clay Content Mapping at Large Scales Using Multispectral (VNIR-SWIR) ASTER Data. *Int. J. Remote Sens.* **2019**, *40*, 1506–1533. [[CrossRef](#)]
131. Lagacherie, P.; Arrouays, D.; Bourennane, H.; Gomez, C.; Nkuba-Kasanda, L. Analysing the Impact of Soil Spatial Sampling on the Performances of Digital Soil Mapping Models and Their Evaluation: A Numerical Experiment on Quantile Random Forest Using Clay Contents Obtained from Vis-NIR-SWIR Hyperspectral Imagery. *Geoderma* **2020**, *375*, 114503. [[CrossRef](#)]
132. Lagacherie, P.; Arrouays, D.; Bourennane, H.; Gomez, C.; Martin, M.; Saby, N.P.A. How Far Can the Uncertainty on a Digital Soil Map Be Known?: A Numerical Experiment Using Pseudo Values of Clay Content Obtained from Vis-SWIR Hyperspectral Imagery. *Geoderma* **2019**, *337*, 1320–1328. [[CrossRef](#)]
133. Wigneron, J.; Kerr, Y.; Waldteufel, P.; Saleh, K.; Escorihuela, M.; Richaume, P.; Ferrazzoli, P.; de Rosnay, P.; Gurney, R.; Calvet, J.; et al. L-Band Microwave Emission of the Biosphere (L-MEB) Model: Description and Calibration against Experimental Data Sets over Crop Fields. *Remote Sens. Environ.* **2007**, *107*, 639–655. [[CrossRef](#)]
134. Shellito, P.J.; Small, E.E.; Cosh, M.H. Calibration of Noah Soil Hydraulic Property Parameters Using Surface Soil Moisture from SMOS and Basinwide In Situ Observations. *J. Hydrometeorol.* **2016**, *17*, 2275–2292. [[CrossRef](#)]
135. Lacoste, M.; Lemerrier, B.; Walter, C. Regional Mapping of Soil Parent Material by Machine Learning Based on Point Data. *Geomorphology* **2011**, *133*, 90–99. [[CrossRef](#)]
136. Samuel-Rosa, A.; Heuvelink, G.B.M.; Vasques, G.M.; Anjos, L.H.C. Do More Detailed Environmental Covariates Deliver More Accurate Soil Maps? *Geoderma* **2015**, *243–244*, 214–227. [[CrossRef](#)]
137. Brus, D.J. *Spatial Sampling with R*, 1st ed.; Chapman and Hall/CRC: Boca Raton, FL, USA, 2022; ISBN 978-1-00-325894-0.
138. Mulder, V.L.; Lacoste, M.; Richer-de-Forges, A.C.; Martin, M.P.; Arrouays, D. National versus Global Modelling the 3D Distribution of Soil Organic Carbon in Mainland France. *Geoderma* **2016**, *263*, 16–34. [[CrossRef](#)]
139. Lemerrier, B.; Lagacherie, P.; Amelin, J.; Sauter, J.; Pichelin, P.; Richer-de-Forges, A.C.; Arrouays, D. Multiscale Evaluations of Global, National and Regional Digital Soil Mapping Products in France. *Geoderma* **2022**, *425*, 116052. [[CrossRef](#)]
140. Chen, S.; Mulder, V.L.; Martin, M.P.; Walter, C.; Lacoste, M.; Richer-de-Forges, A.C.; Saby, N.P.A.; Loiseau, T.; Hu, B.; Arrouays, D. Probability Mapping of Soil Thickness by Random Survival Forest at a National Scale. *Geoderma* **2019**, *344*, 184–194. [[CrossRef](#)]
141. Loiseau, T.; Arrouays, D.; Richer-de-Forges, A.C.; Lagacherie, P.; Ducommun, C.; Minasny, B. Density of Soil Observations in Digital Soil Mapping: A Study in the Mayenne Region, France. *Geoderma Reg.* **2021**, *24*, e00358. [[CrossRef](#)]
142. McKenzie, N.J.; Ryan, P.J. Spatial Prediction of Soil Properties Using Environmental Correlation. *Geoderma* **1999**, *89*, 67–94. [[CrossRef](#)]
143. Arrouays, D.; Leenaars, J.G.B.; Richer-de-Forges, A.C.; Adhikari, K.; Ballabio, C.; Greve, M.; Grundy, M.; Guerrero, E.; Hempel, J.; Hengl, T.; et al. Soil Legacy Data Rescue via GlobalSoilMap and Other International and National Initiatives. *GeoResJ* **2017**, *14*, 1–19. [[CrossRef](#)]
144. Grinand, C.; Arrouays, D.; Laroche, B.; Martin, M.P. Extrapolating Regional Soil Landscapes from an Existing Soil Map: Sampling Intensity, Validation Procedures, and Integration of Spatial Context. *Geoderma* **2008**, *143*, 180–190. [[CrossRef](#)]
145. Lagacherie, P.; Legros, J.P.; Burfough, P.A. A Soil Survey Procedure Using the Knowledge of Soil Pattern Established on a Previously Mapped Reference Area. *Geoderma* **1995**, *65*, 283–301. [[CrossRef](#)]
146. Nauman, T.W.; Thompson, J.A. Semi-Automated Disaggregation of Conventional Soil Maps Using Knowledge Driven Data Mining and Classification Trees. *Geoderma* **2014**, *213*, 385–399. [[CrossRef](#)]
147. Vincent, S.; Lemerrier, B.; Berthier, L.; Walter, C. Spatial Disaggregation of Complex Soil Map Units at the Regional Scale Based on Soil-Landscape Relationships. *Geoderma* **2018**, *311*, 130–142. [[CrossRef](#)]
148. Richer-de-Forges, A.C.; Arrouays, D.; Poggio, L.; Chen, S.; Lacoste, M.; Minasny, B. Hand-Feel Soil Texture Observations to Evaluate the Accuracy of Digital Soil Maps for Local Prediction of Particle Size Distribution. A Case Study in Central France. *Pedosphere* **2022**, in press. [[CrossRef](#)]
149. Raju, S.; Chanzy, A.; Wigneron, J.-P.; Calvet, J.-C.; Kerr, Y.; Laguerre, L. Soil Moisture and Temperature Profile Effects on Microwave Emission at Low Frequencies. *Remote Sens. Environ.* **1995**, *54*, 85–97. [[CrossRef](#)]
150. Wigneron, J.; Schmugge, T.; Chanzy, A.; Calvet, J.; Kerr, Y. Use of Passive Microwave Remote Sensing to Monitor Soil Moisture. *Agronomie* **1998**, *18*, 27–43. [[CrossRef](#)]
151. Wigneron, J.; Ferrazzoli, P.; Calvet, J.; Kerr, Y.; Bertuzzi, P. A Parametric Study on Passive and Active Microwave Observations over a Soybean Crop. *IEEE Trans. Geosci. Remote Sens.* **1999**, *37*, 2728–2733. [[CrossRef](#)]
152. Wigneron, J.; Laguerre, L.; Kerr, Y. A Simple Parameterization of the L-Band Microwave Emission from Rough Agricultural Soils. *IEEE Trans. Geosci. Remote Sens.* **2001**, *39*, 1697–1707. [[CrossRef](#)]
153. Wigneron, J.; Jackson, T.; O'Neill, P.; De Lannoy, G.; de Rosnay, P.; Walker, J.; Ferrazzoli, P.; Mironov, V.; Bircher, S.; Grant, J.; et al. Modelling the Passive Microwave Signature from Land Surfaces: A Review of Recent Results and Application to the L-Band SMOS & SMAP Soil Moisture Retrieval Algorithms. *Remote Sens. Environ.* **2017**, *192*, 238–262. [[CrossRef](#)]
154. Cros, S.; Chanzy, A.; Pellarin, T.; Calvet, J.-C.; Wigneron, J.-P. Using Optical Satellite Based Data to Improve Soil Moisture Retrieval from SMOS Mission. In Proceedings of the 2006 IEEE International Symposium on Geoscience and Remote Sensing, Denver, CO, USA, 31 July–4 August 2006; p. 2021.
155. Escorihuela, M.; Chanzy, A.; Wigneron, J.; Kerr, Y. Effective Soil Moisture Sampling Depth of L-Band Radiometry: A Case Study. *Remote Sens. Environ.* **2010**, *114*, 995–1001. [[CrossRef](#)]

156. Kerr, Y.; Al-Yaari, A.; Rodriguez-Fernandez, N.; Parrens, M.; Molero, B.; Leroux, D.; Bircher, S.; Mahmoodi, A.; Mialon, A.; Richaume, P.; et al. Overview of SMOS Performance in Terms of Global Soil Moisture Monitoring after Six Years in Operation. *Remote Sens. Environ.* **2016**, *180*, 40–63. [[CrossRef](#)]
157. Baghdadi, N.; El Hajj, M.; Choker, M.; Zribi, M.; Bazzi, H.; Vaudour, E.; Gilliot, J.; Bousbih, S.; Mwampongo, D. Potential of Sentinel-1 for Estimating the Soil Roughness over Agricultural Soils. In Proceedings of the IGARSS 2018—2018 IEEE International Geoscience and Remote Sensing Symposium, Valencia, Spain, 22–27 July 2018; pp. 7516–7519.
158. Al-Yaari, A.; Ducharne, A.; Cheruy, F.; Crow, W.; Wigneron, J. Satellite-Based Soil Moisture Provides Missing Link between Summertime Precipitation and Surface Temperature Biases in CMIP5 Simulations over Conterminous United States. *Sci. Rep.* **2019**, *9*, 1657. [[CrossRef](#)]
159. Gruber, A.; de Lannoy, G.; Albergel, C.; Al-yaari, A.; Brocca, L.; Calvet, J.-C.; Colliander, A.; Cosh, M.; Crow, W.T.; Dorigo, W.; et al. Validation Practices for Satellite Soil Moisture Retrievals: What Are (the) Errors? *Remote Sens. Environ.* **2020**, *244*, 111806. [[CrossRef](#)]
160. Wigneron, J.-P.; Kerr, Y.; Chanzy, A.; Jin, Y.-Q. Inversion of Surface Parameters from Passive Microwave Measurements over a Soybean Field. *Remote Sens. Environ.* **1993**, *46*, 61–72. [[CrossRef](#)]
161. Wigneron, J.; Chanzy, A.; Calvet, J.; Bruguier, W. A Simple Algorithm to Retrieve Soil-Moisture and Vegetation Biomass Using Passive Microwave Measurements over Crop Fields. *Remote Sens. Environ.* **1995**, *51*, 331–341. [[CrossRef](#)]
162. Wigneron, J.; Waldteufel, P.; Chanzy, A.; Calvet, J.; Kerr, Y. Two-Dimensional Microwave Interferometer Retrieval Capabilities over Land Surfaces (SMOS Mission). *Remote Sens. Environ.* **2000**, *73*, 270–282. [[CrossRef](#)]
163. Kerr, Y.; Waldteufel, P.; Wigneron, J.; Martinuzzi, J.; Font, J.; Berger, M. Soil Moisture Retrieval from Space: The Soil Moisture and Ocean Salinity (SMOS) Mission. *IEEE Trans. Geosci. Remote Sens.* **2001**, *39*, 1729–1735. [[CrossRef](#)]
164. Baghdadi, N.; El Hajj, M.; Choker, M.; Zribi, M.; Bazzi, H.; Vaudour, E.; Gilliot, J.-M.; Ebengo, D. Potential of Sentinel-1 Images for Estimating the Soil Roughness over Bare Agricultural Soils. *Water* **2018**, *10*, 131. [[CrossRef](#)]
165. Albergel, C.; Rudiger, C.; Pellarin, T.; Calvet, J.; Fritz, N.; Froissard, F.; Suquia, D.; Petitpa, A.; Piguet, B.; Martin, E. From Near-Surface to Root-Zone Soil Moisture Using an Exponential Filter: An Assessment of the Method Based on in-Situ Observations and Model Simulations. *Hydrol. Earth Syst. Sci.* **2008**, *12*, 1323–1337. [[CrossRef](#)]
166. Sadeghi, M.; Babaeian, E.; Tuller, M.; Jones, S.B. The Optical Trapezoid Model: A Novel Approach to Remote Sensing of Soil Moisture Applied to Sentinel-2 and Landsat-8 Observations. *Remote Sens. Environ.* **2017**, *198*, 52–68. [[CrossRef](#)]
167. Petropoulos, G.P.; Ireland, G.; Barrett, B. Surface Soil Moisture Retrievals from Remote Sensing: Current Status, Products & Future Trends. *Phys. Chem. Earth* **2015**, *83–84*, 36–56. [[CrossRef](#)]
168. Sandholt, I.; Rasmussen, K.; Andersen, J. A Simple Interpretation of the Surface Temperature/Vegetation Index Space for Assessment of Surface Moisture Status. *Remote Sens. Environ.* **2002**, *79*, 213–224. [[CrossRef](#)]
169. Hassan-Esfahani, L.; Torres-Rua, A.; Jensen, A.; Mckee, M. Spatial Root Zone Soil Water Content Estimation in Agricultural Lands Using Bayesian-Based Artificial Neural Networks and High-Resolution Visual, NIR, and Thermal Imagery: Remote Sensing of Agricultural Soil Moisture Using UAV. *Irrig. Drain.* **2017**, *66*, 273–288. [[CrossRef](#)]
170. Li, F.; Crow, W.T.; Kustas, W.P. Towards the Estimation Root-Zone Soil Moisture via the Simultaneous Assimilation of Thermal and Microwave Soil Moisture Retrievals. *Adv. Water Resour.* **2010**, *33*, 201–214. [[CrossRef](#)]
171. King, C.; Lecomte, V.; Le Bissonnais, Y.; Baghdadi, N.; Souchere, V.; Cerdan, O. Remote-Sensing Data as an Alternative Input for the “STREAM” Runoff Model. *CATENA* **2005**, *62*, 125–135. [[CrossRef](#)]
172. Bretar, F.; Arab-Sedze, M.; Champion, J.; Pierrot-Deseilligny, M.; Heggy, E.; Jacquemoud, S. An Advanced Photogrammetric Method to Measure Surface Roughness: Application to Volcanic Terrains in the Piton de La Fournaise, Reunion Island. *Remote Sens. Environ.* **2013**, *135*, 1–11. [[CrossRef](#)]
173. Gilliot, J.M.; Vaudour, E.; Michelin, J. Soil Surface Roughness Measurement: A New Fully Automatic Photogrammetric Approach Applied to Agricultural Bare Fields. *Comput. Electron. Agric.* **2017**, *134*, 63–78. [[CrossRef](#)]
174. Parrens, M.; Wigneron, J.; Richaume, P.; Mialon, A.; Al Bitar, A.; Fernandez-Moran, R.; Al-Yaari, A.; Kerr, Y. Global-Scale Surface Roughness Effects at L-Band as Estimated from SMOS Observations. *Remote Sens. Environ.* **2016**, *181*, 122–136. [[CrossRef](#)]
175. Baghdadi, N.; Cerdan, O.; Zribi, M.; Auzet, V.; Darboux, F.; El Hajj, M.; Kheir, R. Operational Performance of Current Synthetic Aperture Radar Sensors in Mapping Soil Surface Characteristics in Agricultural Environments: Application to Hydrological and Erosion Modelling. *Hydrol. Process.* **2008**, *22*, 9–20. [[CrossRef](#)]
176. Paustian, K.; Lehmann, J.; Ogle, S.; Reay, D.; Robertson, G.P.; Smith, P. Climate-Smart Soils. *Nature* **2016**, *532*, 49–57. [[CrossRef](#)]
177. Minasny, B.; Malone, B.P.; McBratney, A.B.; Angers, D.A.; Arrouays, D.; Chambers, A.; Chaplot, V.; Chen, Z.-S.; Cheng, K.; Das, B.S.; et al. Soil Carbon 4 per Mille. *Geoderma* **2017**, *292*, 59–86. [[CrossRef](#)]
178. Minasny, B.; Arrouays, D.; McBratney, A.B.; Angers, D.A.; Chambers, A.; Chaplot, V.; Chen, Z.-S.; Cheng, K.; Das, B.S.; Field, D.J.; et al. Rejoinder to Comments on Minasny et al., 2017 Soil Carbon 4 per Mille *Geoderma* **2018**, *309*, 124–129. [[CrossRef](#)]
179. Chenu, C.; Angers, D.A.; Barré, P.; Derrien, D.; Arrouays, D.; Balesdent, J. Increasing Organic Stocks in Agricultural Soils: Knowledge Gaps and Potential Innovations. *Soil Tillage Res.* **2019**, *188*, 41–52. [[CrossRef](#)]
180. Angelopoulou, T.; Tziolas, N.; Balafoutis, A.; Zalidis, G.; Bochtis, D. Remote Sensing Techniques for Soil Organic Carbon Estimation: A Review. *Remote Sens.* **2019**, *11*, 676. [[CrossRef](#)]

181. Vaudour, E.; Gholizadeh, A.; Castaldi, F.; Saberioon, M.; Borůvka, L.; Urbina-Salazar, D.; Fouad, Y.; Arrouays, D.; Richer-De-Forges, A.; Biney, J.; et al. Satellite Imagery to Map Topsoil Organic Carbon Content over Cultivated Areas: An Overview. *Remote Sens.* **2022**, *14*, 2917. [CrossRef]
182. Vaudour, E.; Gomez, C.; Loiseau, T.; Baghdadi, N.; Loubet, B.; Arrouays, D.; Ali, L.; Lagacherie, P. The Impact of Acquisition Date on the Prediction Performance of Topsoil Organic Carbon from Sentinel-2 for Croplands. *Remote Sens.* **2019**, *11*, 2143. [CrossRef]
183. Castaldi, F.; Chabrillat, S.; Don, A.; van Wesemael, B. Soil Organic Carbon Mapping Using LUCAS Topsoil Database and Sentinel-2 Data: An Approach to Reduce Soil Moisture and Crop Residue Effects. *Remote Sens.* **2019**, *11*, 2121. [CrossRef]
184. Vaudour, E.; Gilliot, J.M.; Bel, L.; Lefevre, J.; Chehdi, K. Regional Prediction of Soil Organic Carbon Content over Temperate Croplands Using Visible Near-Infrared Airborne Hyperspectral Imagery and Synchronous Field Spectra. *Int. J. Appl. Earth Obs. Geoinf.* **2016**, *49*, 24–38. [CrossRef]
185. Gomez, C.; Rossel, R.; McBratney, A. Soil Organic Carbon Prediction by Hyperspectral Remote Sensing and Field Vis-NIR Spectroscopy: An Australian Case Study. *Geoderma* **2008**, *146*, 403–411. [CrossRef]
186. Vaudour, E.; Bel, L.; Gilliot, J.M.; Coquet, Y.; Hadjar, D.; Cambier, P.; Michelin, J.; Houot, S. Potential of SPOT Multispectral Satellite Images for Mapping Topsoil Organic Carbon Content over Peri-Urban Croplands. *Soil Sci. Soc. Am. J.* **2013**, *77*, 2122–2139. [CrossRef]
187. Berthier, L.; Pitres, J.C.; Vaudour, E. Prédiction Spatiale Des Teneurs En Carbone Organique Des Sols Par Spectroscopie Visible-Proche Infrarouge et Télédétection Satellitale SPOT. Exemple Au Niveau d'un Périmètre d'alimentation En Eau Potable En Beauce. *Etude Gest. Sols* **2008**, *15*, 161–172.
188. Bsaiibes, A.; Courault, D.; Baret, F.; Weiss, M.; Oliosio, A.; Jacob, F.; Hagolle, O.; Marloie, O.; Bertrand, N.; Desfond, V.; et al. Albedo and LAI Estimates from FORMOSAT-2 Data for Crop Monitoring. *Remote Sens. Environ.* **2009**, *113*, 716–729. [CrossRef]
189. Gomez, C.; Lagacherie, P.; Coulouma, G. Continuum Removal versus PLSR Method for Clay and Calcium Carbonate Content Estimation from Laboratory and Airborne Hyperspectral Measurements. *Geoderma* **2008**, *148*, 141–148. [CrossRef]
190. Nouri, M.; Gomez, C.; Gorretta, N.; Roger, J.M. Clay Content Mapping from Airborne Hyperspectral Vis-NIR Data by Transferring a Laboratory Regression Model. *Geoderma* **2017**, *298*, 54–66. [CrossRef]
191. Bousbih, S.; Zribi, M.; Pelletier, C.; Gorrab, A.; Lili-Chabaane, Z.; Baghdadi, N.; Ben Aissa, N.; Mougénot, B. Soil Texture Estimation Using Radar and Optical Data from Sentinel-1 and Sentinel-2. *Remote Sens.* **2019**, *11*, 1520. [CrossRef]
192. Gomez, C.; Dharumarajan, S.; Féret, J.-B.; Lagacherie, P.; Ruiz, L.; Sekhar, M. Use of Sentinel-2 Time-Series Images for Classification and Uncertainty Analysis of Inherent Biophysical Property: Case of Soil Texture Mapping. *Remote Sens.* **2019**, *11*, 565. [CrossRef]
193. Gomez, C.; Vaudour, E.; Féret, J.-B.; de Boissieu, F.; Dharumarajan, S. Topsoil Clay Content Mapping in Croplands from Sentinel-2 Data: Influence of Atmospheric Correction Methods across a Season Time Series. *Geoderma* **2022**, *423*, 115959. [CrossRef]
194. Chabrillat, S.; Goetz, A.F.H.; Krosley, L.; Olsen, H.W. Use of Hyperspectral Images in the Identification and Mapping of Expansive Clay Soils and the Role of Spatial Resolution. *Remote Sens. Environ.* **2002**, *82*, 431–445. [CrossRef]
195. Escadafal, R.; Pouget, M. Cartographie Des Formations Superficielles En Zone Aride (Tunisie Méridionale) Avec Landsat TM. *Photo-Interprétation* **1987**, *4*, 9–15.
196. de Martonne, E. Photogrammétrie et photographie aérienne: À propos du congrès et de l'exposition internationale de photogrammétrie. *Ann. Géographie* **1935**, *44*, 65–70. [CrossRef]
197. Lagacherie, P.; Robbez-Masson, J.M.; Nguyen-The, N.; Barthès, J.P. Mapping of Reference Area Representativity Using a Mathematical Soilscap Distance. *Geoderma* **2001**, *101*, 105–118. [CrossRef]
198. Hamdi-Aïssa, B.; Girard, M.-C. Utilisation de La Télédétection En Régions Sahariennes, Pour l'analyse et l'extrapolation Spatiale Des Pédopaysages. *Sci. Chang. Planétaires Sécheresse* **2000**, *11*, 179–188.
199. Girard, M.-C. Recherche d'une Modélisation En Vue d'une Représentation Spatiale de La Couverture Pédologique. Ph.D. Thesis, Institut National Agronomique Paris-Grignon, Paris, France, 1983.
200. Girard, M.-C.; King, D. Un Algorithme Interactif Pour La Classification Des Horizons de La Couverture Pédologique. *Sci. Sol* **1988**, *26*, 81–102.
201. Girard, M.; Mougénot, B.; Rananoson, A. *Présentation d'un Modèle d'organisation et D'analyse de La Structure Des Informations Spatialisées: OASIS*; ORSTOM: Paris, France, 1990.
202. Robbez-Masson, J.-M.; Foltete, J.-C.; Cabello, L.; Flitti, M. Prise en compte du contexte spatial dans l'instrumentation de la notion de paysage—Application à une segmentation géographique assistée. *Rev. Int. Géomatique* **1999**, *9*, 173–195.
203. Robbez-Masson, J.-M. Reconnaissance et Délimitation de Motifs D'organisation Spatiale—Application à la Cartographie de Pédopaysages. Ph.D. Thesis, Ecole Nationale Supérieure Agronomique de Montpellier, Montpellier, France, 1994.
204. Lehmann, S.; Bégon, J.-C.; Eimberck, M.; Daroussin, J.; Wynns, R.; Arrouays, D. Utilisation du logiciel CLAPAS pour l'aide à la délimitation de pédopaysages. Un test sur la carte des sols de Mirande (Gers, France). *Etude Gest. Sols* **2007**, *14*, 135–151.
205. Bourget, É.; Le Dû-Blayo, L. Définition d'unités Paysagères Par Télédétection En Bretagne: Méthodes et Critiques. *Norv. J. Geogr.* **2010**, *216*, 69–83. [CrossRef]
206. Le Dû-Blayo, L.; Gouery, P.; Corpetti, T.; Michel, K.; Lemerrier, B.; Walter, C. Improving the Input of Remotely-Sensed Data and Information into Digital Soil Maps. In *Digital Soil Mapping with Limited Soil Data*; Hartemink, A.E., Ed.; Developments in Soil Science; Elsevier: Amsterdam, The Netherlands, 2008; pp. 337–348.
207. United States Geological Survey. Landsat Data Access. 2023. Available online: <https://www.usgs.gov/landsat-missions/landsat-data-access> (accessed on 29 May 2023).

208. IPCC. *Climate Change 2007: Synthesis Report. Contribution of Working Groups I, II and III to the Fourth Assessment Report of the Intergovernmental Panel on Climate Change*; Core Writing Team, Pachauri, R.K., Reisinger, A., Eds.; IPCC: Geneva, Switzerland, 2007; 104p.
209. Stenberg, B.; Viscarra Rossel, R.A.; Mouazen, A.M.; Wetterlind, J. Visible and Near Infrared Spectroscopy in Soil Science. *Adv. Agron.* **2010**, *107*, 163–215. [[CrossRef](#)]
210. Barthès, B.G.; Chotte, J. Infrared Spectroscopy Approaches Support Soil Organic Carbon Estimations to Evaluate Land Degradation. *Land Degrad. Dev.* **2021**, *32*, 310–322. [[CrossRef](#)]
211. European Commission. *Communication from the Commission to the European Parliament, the Council, the European Economic and Social Committee and the Committee of the Regions. EU Soil Strategy for 2030. Reaping the Benefits of Healthy Soils for People, Food, Nature and Climate*; European Commission: Brussels, Belgium, 2021.
212. Smith, P. Monitoring and Verification of Soil Carbon Changes under Article 3.4 of the Kyoto Protocol. *Soil Use Manag.* **2006**, *20*, 264–270. [[CrossRef](#)]
213. Smith, P.; Soussana, J.-F.; Angers, D.; Schipper, L.; Chenu, C.; Rasse, D.P.; Batjes, N.H.; van Egmond, F.; Mcneill, S.; Kuhnert, M.; et al. How to Measure, Report and Verify Soil Carbon Change to Realise the Potential of Soil Carbon Sequestration for Atmospheric Greenhouse Gas Removal. *Glob. Change Biol.* **2020**, *26*, 219–241. [[CrossRef](#)]
214. Soussana, J.-F.; Lutfalla, S.; Ehrhardt, F.; Rosenstock, T.; Lamanna, C.; Havlík, P.; Richards, M.; Wollenberg, E.L.; Chotte, J.-L.; Torquebiau, E.; et al. Matching Policy and Science: Rationale for the ‘4 per 1000—Soils for Food Security and Climate’ Initiative. *Soil Tillage Res.* **2019**, *188*, 3–15. [[CrossRef](#)]
215. Martin, M.P.; Dimassi, B.; Román Dobarco, M.; Guenet, B.; Arrouays, D.; Angers, D.A.; Blache, F.; Huard, F.; Soussana, J.; Pellerin, S. Feasibility of the 4 per 1000 Aspirational Target for Soil Carbon: A Case Study for France. *Glob. Change Biol.* **2021**, *27*, 2458–2477. [[CrossRef](#)] [[PubMed](#)]
216. Rabot, E.; Keller, C.; Ambrosi, J.-P.; Robert, S. Revue des méthodes multiparamétriques pour l’estimation de la qualité des sols, dans le cadre de l’aménagement du territoire. *Etude Gest. Sols* **2017**, *24*, 59–72.
217. Cabral, P.; Feger, C.; Levrel, H.; Chambolle, M.; Basque, D. Assessing the Impact of Land-Cover Changes on Ecosystem Services: A First Step toward Integrative Planning in Bordeaux, France. *Ecosyst. Serv.* **2016**, *22*, 318–327. [[CrossRef](#)]
218. Stoian, A.; Poulain, V.; Inglada, J.; Poughon, V.; Derksen, D. Land Cover Maps Production with High Resolution Satellite Image Time Series and Convolutional Neural Networks: Adaptations and Limits for Operational Systems. *Remote Sens.* **2019**, *11*, 1986. [[CrossRef](#)]
219. Cerdan, O.; Delmas, M.; Négrel, P.; Mouchel, J.-M.; Petelet-Giraud, E.; Salvador-Blanes, S.; Degan, F. Contribution of Diffuse Hillslope Erosion to the Sediment Export of French Rivers. *Comptes Rendus Geosci.* **2012**, *344*, 636–645. [[CrossRef](#)]
220. Gay, A.; Cerdan, O.; Delmas, M.; Desmet, M. Variability of Suspended Sediment Yields within the Loire River Basin (France). *J. Hydrol.* **2014**, *519*, 1225–1237. [[CrossRef](#)]
221. Patault, E.; Ledun, J.; Landemaine, V.; Soullignac, A.; Richet, J.-B.; Fournier, M.; Ouvry, J.-F.; Cerdan, O.; Laignel, B. Analysis of Off-Site Economic Costs Induced by Runoff and Soil Erosion: Example of Two Areas in the Northwestern European Loess Belt for the Last Two Decades (Normandy, France). *Land Use Policy* **2021**, *108*, 105541. [[CrossRef](#)]
222. King, C.; Baghdadi, N.; Lecomte, V.; Cerdan, O. The Application of Remote-Sensing Data to Monitoring and Modelling of Soil Erosion. *CATENA* **2005**, *62*, 79–93. [[CrossRef](#)]
223. Desprats, J.; Raclot, D.; Rousseau, M.; Cerdan, O.; Garcin, M.; Le Bissonnais, Y.; Ben Slimane, A.; Fouche, J.; Monfort-Clement, D. Mapping Linear Erosion Features Using High and Very High Resolution Satellite Imagery. *Land Degrad. Dev.* **2013**, *24*, 22–32. [[CrossRef](#)]
224. Pineux, N.; Lisein, J.; Swerts, G.; Biëlders, C.L.; Lejeune, P.; Colinet, G.; Degré, A. Can DEM Time Series Produced by UAV Be Used to Quantify Diffuse Erosion in an Agricultural Watershed? *Geomorphology* **2017**, *280*, 122–136. [[CrossRef](#)]
225. Abass Saley, A.; Baratoux, D.; Baratoux, L.; Ahoussi, K.E.; Yao, K.A.; Kouamé, K.J. Evolution of the Koma Bangou Gold Panning Site (Niger) From 1984 to 2020 Using Landsat Imagery. *Earth Space Sci.* **2021**, *8*, e2021EA001879. [[CrossRef](#)]
226. Hong, Y.; Shen, R.; Cheng, H.; Chen, S.; Chen, Y.; Guo, L.; He, J.; Liu, Y.; Yu, L.; Liu, Y. Cadmium Concentration Estimation in Pen-Urban Agricultural Soils: Using Reflectance Spectroscopy, Soil Auxiliary Information, or a Combination of Both? *Geoderma* **2019**, *354*, 113875. [[CrossRef](#)]
227. Lever, V.; Foucher, P.; Briottet, X.; Poutier, L.; Deliot, P.; Viallefont, F.; Dubucq, D. *IEEE Estimation of Hydrocarbon Content in Airborne Hyperspectral Images by a PLS Regression Model Calibrated on Synthetic Airborne Spectral Database*; National Office for Aerospace Studies & Research (ONERA): Palaiseau, France, 2015; pp. 1737–1740.
228. Lever, V.; Foucher, P.; Briottet, X.; Dubucq, D.; Carrio, R.; Poutier, L.; Achard, V.; Deliot, P. Joint Lab, Field and Airborne Spectral Database for the Quantification of Soil Hydrocarbon Content. In Proceedings of the National Office for Aerospace Studies & Research (ONERA), Los Angeles, CA, USA, 21–24 August 2016.
229. Lassalle, G.; Fabre, S.; Credo, A.; Dubucq, D.; Elger, A. Monitoring Oil Contamination in Vegetated Areas with Optical Remote Sensing: A Comprehensive Review. *J. Hazard. Mater.* **2020**, *393*, 122427. [[CrossRef](#)]
230. Faulques, E.; Kalashnyk, N.; Massuyeau, F.; Perry, D. Spectroscopic Markers for Uranium (VI) Phosphates: A Vibronic Study. *RSC Adv.* **2015**, *5*, 71219–71227. [[CrossRef](#)]
231. Xu, D.; Zhao, R.; Li, S.; Chen, S.; Jiang, Q.; Zhou, L.; Shi, Z. Multi-Sensor Fusion for the Determination of Several Soil Properties in the Yangtze River Delta, China. *Eur. J. Soil Sci.* **2019**, *70*, 162–173. [[CrossRef](#)]



232. Martelet, G.; Drufin, S.; Tourliere, B.; Saby, N.P.A.; Perrin, J.; Deparis, J.; Prognon, F.; Jolivet, C.; Ratié, C.; Arrouays, D. Regional Regolith Parameter Prediction Using the Proxy of Airborne Gamma Ray Spectrometry. *Vadose Zone J.* **2013**, *12*, 1–14. [[CrossRef](#)]
233. Wetterlind, J.; Tourliere, B.; Martelet, G.; Deparis, J.; Saby, N.; Richer de Forges, A.; Arrouays, D. Are There Any Effects of the Agricultural Use of Chemical Fertiliser on Elements Detected by Airborne Gamma-Spectrometric Surveys? *Geoderma* **2012**, *173*, 34–41. [[CrossRef](#)]
234. Lassalle, G.; Fabre, S.; Credo, A.; Dubucq, D.; de Souza Filho, C.R. Remote Sensing of Oil in Vegetated Regions: An Overview of Recent Advances and Future Challenges Toward Operational Applications. In Proceedings of the IGARSS 2020—2020 IEEE International Geoscience and Remote Sensing Symposium, Waikoloa, HI, USA, 26 September–2 October 2020; pp. 4045–4048.
235. Achard, V.; Foucher, P.; Dubucq, D. Hydrocarbon Pollution Detection and Mapping Based on the Combination of Various Hyperspectral Imaging Processing Tools. *Remote Sens.* **2021**, *13*, 1020. [[CrossRef](#)]
236. Tabet, D.; Vidal, A.; Zimmer, D.; Asif, S.; Aslam, M.; Kuper, M.; Strosser, P. Soil Salinity Characterisation in SPOT Images: A Case Study in One Irrigation System of the Punjab, Pakistan. In Proceedings of the Seventh International Symposium on Physical Measurements and Signatures in Remote Sensing, Courchevel, France, 7–11 April 1997; pp. 795–800.
237. Douaoui, A.; Nicolas, H.; Walter, C. Detecting Salinity Hazards within a Semiarid Context by Means of Combining Soil and Remote-Sensing Data. *Geoderma* **2006**, *134*, 217–230. [[CrossRef](#)]
238. Saby, N.P.A.; Arrouays, D.; Antoni, V.; Lemercier, B.; Follain, S.; Walter, C.; Schwartz, C. Changes in Soil Organic Carbon in a Mountainous French Region, 1990–2004. *Soil Use Manag.* **2008**, *24*, 254–262. [[CrossRef](#)]
239. Lagacherie, P.; Gomez, C.; Bailly, J.; Baret, F.; Coulouma, G. The Use of Hyperspectral Imagery for Digital Soil Mapping in Mediterranean Areas. In *Digital Soil Mapping*; Boettinger, J., Howell, D., Moore, A., Hartemink, A., Kienast-Brown, S., Eds.; Springer: Dordrecht, The Netherlands, 2010; Volume 2, pp. 93–102.
240. Lagacherie, P.; Gomez, C. Vis-NIR-SWIR Remote Sensing Products as New Soil Data for Digital Soil Mapping. In *PEDOMETRICS*; McBratney, A., Minasny, B., Stockmann, U., Eds.; Springer: Berlin/Heidelberg, Germany, 2018; pp. 415–437. ISBN 2352-4774.
241. Loiseau, T.; Chen, S.; Mulder, V.L.; Román Dobarco, M.; Richer-de-Forges, A.C.; Lehmann, S.; Bourennane, H.; Saby, N.P.A.; Martin, M.P.; Vaudour, E.; et al. Satellite Data Integration for Soil Clay Content Modelling at a National Scale. *Int. J. Appl. Earth Obs. Geoinf.* **2019**, *82*, 101905. [[CrossRef](#)]
242. Ouerghemmi, W.; Gomez, C.; Naceur, S.; Lagacherie, P. Semi-Blind Source Separation for the Estimation of the Clay Content over Semi-Vegetated Areas Using VNIR/SWIR Hyperspectral Airborne Data. *Remote Sens. Environ.* **2016**, *181*, 251–263. [[CrossRef](#)]
243. Urbina-Salazar, D.; Vaudour, E.; Richer-de-Forges, A.C.; Chen, S.; Martelet, G.; Baghdadi, N.; Arrouays, D. Sentinel-2 and Sentinel-1 Bare Soil Temporal Mosaics of 6-Year Periods for Soil Organic Carbon Content Mapping in Central France. *Remote Sens.* **2023**, *15*, 2410. [[CrossRef](#)]
244. Glinka, K.D. *Dokuchaev's Ideas in the Development of Pedology and the Cognate Sciences*; The Academy: Saint Petersburg, Russia, 1927.
245. Gerasimov, I.P. VV Dokuchaev's Doctrine of Natural Zones. *Pochvovedenie* **1946**, *6*, 353–360.
246. Gregoryev, A.A.; Gerasimov, I.P. (Eds.) *VV Dokuchaev and Geography*; Academy of Science: Moscow, Russia, 1946.
247. Simonson, R.W. Early Teaching in USA of Dokuchaev Factors of Soil Formation. *Soil Sci. Soc. Am. J.* **1997**, *61*, 11–16. [[CrossRef](#)]
248. Batjes, N.H. Total Carbon and Nitrogen in the Soils of the World. *Eur. J. Soil Sci.* **1996**, *47*, 151–163. [[CrossRef](#)]
249. Poggio, L.; de Sousa, L.M.; Batjes, N.H.; Heuvelink, G.B.M.; Kempen, B.; Ribeiro, E.; Rossiter, D. SoilGrids 2.0: Producing Soil Information for the Globe with Quantified Spatial Uncertainty. *SOIL* **2021**, *7*, 217–240. [[CrossRef](#)]
250. Martin, M.P.; Wattenbach, M.; Smith, P.; Meersmans, J.; Jolivet, C.; Boulonne, L.; Arrouays, D. Spatial Distribution of Soil Organic Carbon Stocks in France. *Biogeosciences* **2011**, *8*, 1053–1065. [[CrossRef](#)]
251. Meersmans, J.; Martin, M.P.; De Ridder, F.; Lacarce, E.; Wetterlind, J.; De Baets, S.; Le Bas, C.; Louis, B.P.; Orton, T.G.; Bispo, A.; et al. A Novel Soil Organic C Model Using Climate, Soil Type and Management Data at the National Scale in France. *Agron. Sustain. Dev.* **2012**, *32*, 873–888. [[CrossRef](#)]
252. Martin, M.P.; Orton, T.G.; Lacarce, E.; Meersmans, J.; Saby, N.P.A.; Paroissien, J.B.; Jolivet, C.; Boulonne, L.; Arrouays, D. Evaluation of Modelling Approaches for Predicting the Spatial Distribution of Soil Organic Carbon Stocks at the National Scale. *Geoderma* **2015**, *223–225*, 97–107. [[CrossRef](#)]
253. Chen, S.; Arrouays, D.; Angers, D.A.; Chenu, C.; Barré, P.; Martin, M.P.; Saby, N.P.A.; Walter, C. National Estimation of Soil Organic Carbon Storage Potential for Arable Soils: A Data-Driven Approach Coupled with Carbon-Landscape Zones. *Sci. Total Environ.* **2019**, *666*, 355–367. [[CrossRef](#)]
254. Grosset, Y.; Richer-de-Forges, A.C.; Demartini, J.; Saby, N.P.A.; Martin, M.P.; Meersmans, J.; Arrouays, D. Une Analyse Des Facteurs de Contrôle de La Distribution Des Teneurs En Carbone Des Horizons Superficiels Des Sols de Corse. *Etude Gest. Sols* **2011**, *18*, 247–258.
255. Landré, A.; Cornu, S.; Meunier, J.-D.; Guerin, A.; Arrouays, D.; Caubet, M.; Ratié, C.; Saby, N.P.A. Do Climate and Land Use Affect the Pool of Total Silicon Concentration? A Digital Soil Mapping Approach of French Topsoils. *Geoderma* **2020**, *364*, 114175. [[CrossRef](#)]
256. Le Bissonnais, Y.; Montier, C.; Jamagne, M.; Daroussin, J.; King, D. Mapping Erosion Risk for Cultivated Soil in France. *CATENA* **2002**, *46*, 207–220. [[CrossRef](#)]
257. Arrouays, D.; Deslais, W.; Bateau, V. The Carbon Content of Topsoil and Its Geographical Distribution in France. *Soil Use Manag.* **2006**, *17*, 7–11. [[CrossRef](#)]

258. Meersmans, J.; Martin, M.P.; Lacarce, E.; De Baets, S.; Jolivet, C.; Boulonne, L.; Lehmann, S.; Saby, N.P.A.; Bispo, A.; Arrouays, D. A High Resolution Map of French Soil Organic Carbon. *Agron. Sustain. Dev.* **2012**, *32*, 841–851. [[CrossRef](#)]
259. Mulder, V.L.; Lacoste, M.; Richer-de-Forges, A.C.; Arrouays, D. GlobalSoilMap France: High-Resolution Spatial Modelling the Soils of France up to Two Meter Depth. *Sci. Total Environ.* **2016**, *573*, 1352–1369. [[CrossRef](#)]
260. Chen, S.; Martin, M.P.; Saby, N.P.A.; Walter, C.; Angers, D.A.; Arrouays, D. Fine Resolution Map of Top- and Subsoil Carbon Sequestration Potential in France. *Sci. Total Environ.* **2018**, *630*, 389–400. [[CrossRef](#)]
261. Chen, S.; Arrouays, D.; Angers, D.A.; Martin, M.P.; Walter, C. Soil Carbon Stocks under Different Land Uses and the Applicability of the Soil Carbon Saturation Concept. *Soil Tillage Res.* **2019**, *188*, 53–58. [[CrossRef](#)]
262. Villanneau, E.J.; Saby, N.P.A.; Orton, T.G.; Jolivet, C.C.; Boulonne, L.; Caria, G.; Barriuso, E.; Bispo, A.; Briand, O.; Arrouays, D. First Evidence of Large-Scale PAH Trends in French Soils. *Environ. Chem. Lett.* **2013**, *11*, 99–104. [[CrossRef](#)]
263. Froger, C.; Quantin, C.; Bordier, L.; Monvoisin, G.; Evrard, O.; Ayrault, S. Quantification of Spatial and Temporal Variations in Trace Element Fluxes Originating from Urban Areas at the Catchment Scale. *J. Soils Sediments* **2020**, *20*, 4055–4069. [[CrossRef](#)]
264. Froger, C.; Saby, N.P.A.; Jolivet, C.C.; Boulonne, L.; Caria, G.; Freulon, X.; de Fouquet, C.; Roussel, H.; Marot, F.; Bispo, A. Spatial Variations, Origins, and Risk Assessments of Polycyclic Aromatic Hydrocarbons in French Soils. *SOIL* **2021**, *7*, 161–178. [[CrossRef](#)]
265. Mathieu, R.; King, C.; Le Bissonnais, Y. Contribution of Multi-Temporal SPOT Data to the Mapping of a Soil Erosion Index. The Case of the Loamy Plateaux of Northern France. *Soil Technol.* **1997**, *10*, 99–110. [[CrossRef](#)]
266. Souchère, V.; King, C.; Dubreuil, N.; Lecomte-Morel, V.; Le Bissonnais, Y.; Chalal, M. Grassland and Crop Trends: Role of the European Union Common Agricultural Policy and Consequences for Runoff and Soil Erosion. *Environ. Sci. Policy* **2003**, *6*, 7–16. [[CrossRef](#)]
267. Souchère, V.; Cerdan, O.; Ludwig, B.; Le Bissonnais, Y.; Couturier, A.; Papy, F. Modelling Ephemeral Gully Erosion in Small Cultivated Catchments. *CATENA* **2003**, *50*, 489–505. [[CrossRef](#)]
268. Courault, D.; Bertuzzi, P.; Girard, M.-C. Monitoring Surface Changes of Bare Soils Due to Slaking Using Spectral Measurements. *Soil Sci. Soc. Am. J.* **1993**, *57*, 1595–1601. [[CrossRef](#)]
269. Hill, J.; Mégier, J.; Mehl, W. Land Degradation, Soil Erosion and Desertification Monitoring in Mediterranean Ecosystems. *Remote Sens. Rev.* **1995**, *12*, 107–130. [[CrossRef](#)]
270. Cerdan, O.; Bissonnais, Y.L.; Souchère, V.; Martin, P.; Lecomte, V. Sediment Concentration in Interrill Flow: Interactions between Soil Surface Conditions, Vegetation and Rainfall. *Earth Surf. Process. Landf.* **2002**, *27*, 193–205. [[CrossRef](#)]
271. Cerdan, O.; Le Bissonnais, Y.; Couturier, A.; Saby, N. Modelling Interrill Erosion in Small Cultivated Catchments. *Hydrol. Process.* **2002**, *16*, 3215–3226. [[CrossRef](#)]
272. Chen, S.; Richer-de-Forges, A.C.; Leatitia Mulder, V.; Martelet, G.; Loiseau, T.; Lehmann, S.; Arrouays, D. Digital Mapping of the Soil Thickness of Loess Deposits over a Calcareous Bedrock in Central France. *CATENA* **2021**, *198*, 105062. [[CrossRef](#)]
273. Myneni, R.B.; Hall, F.G.; Sellers, P.J.; Marshak, A.L. The Interpretation of Spectral Vegetation Indexes. *IEEE Trans. Geosci. Remote Sens.* **1995**, *33*, 481–486. [[CrossRef](#)]
274. Seguin, B.; Itier, B. Using Midday Surface Temperature to Estimate Daily Evaporation from Satellite Thermal IR Data. *Int. J. Remote Sens.* **1983**, *4*, 371–383. [[CrossRef](#)]
275. Courault, D.; Lagouarde, J.P.; Aloui, B. Evaporation for Maritime Catchment Combining a Meteorological Model with Vegetation Information and Airborne Surface Temperatures. *Agric. For. Meteorol.* **1996**, *82*, 93–117. [[CrossRef](#)]
276. Delogu, E.; Olioso, A.; Alliès, A.; Demarty, J.; Boulet, G. Evaluation of Multiple Methods for the Production of Continuous Evapotranspiration Estimates from TIR Remote Sensing. *Remote Sens.* **2021**, *13*, 1086. [[CrossRef](#)]
277. Román Dobarco, M.; Bourennane, H.; Arrouays, D.; Saby, N.P.A.; Cousin, I.; Martin, M.P. Uncertainty Assessment of Global-SoilMap Soil Available Water Capacity Products: A French Case Study. *Geoderma* **2019**, *344*, 14–39. [[CrossRef](#)]
278. Richer-de-Forges, A.C.; Arrouays, D.; Chen, S.; Román Dobarco, M.; Libohova, Z.; Roudier, P.; Minasny, B.; Bourennane, H. Hand-Feel Soil Texture and Particle-Size Distribution in Central France. Relationships and Implications. *CATENA* **2022**, *213*, 106155. [[CrossRef](#)]
279. Varella, H.; Guérif, M.; Buis, S.; Beaudoin, N. Soil Properties Estimation by Inversion of a Crop Model and Observations on Crops Improves the Prediction of Agro-Environmental Variables. *Eur. J. Agron.* **2010**, *33*, 139–147. [[CrossRef](#)]
280. Ferrant, S.; Bustillo, V.; Burel, E.; Salmon-Monviola, J.; Claverie, M.; Jarosz, N.; Yin, T.; Rivalland, V.; Dedieu, G.; Demarez, V.; et al. Extracting Soil Water Holding Capacity Parameters of a Distributed Agro-Hydrological Model from High Resolution Optical Satellite Observations Series. *Remote Sens.* **2016**, *8*, 154. [[CrossRef](#)]
281. Dewaele, H.; Munier, S.; Albergel, C.; Planque, C.; Laanaia, N.; Carrer, D.; Calvet, J.-C. Parameter Optimisation for a Better Representation of Drought by LSMs: Inverse Modelling vs. Sequential Data Assimilation. *Hydrol. Earth Syst. Sci.* **2017**, *21*, 4861–4878. [[CrossRef](#)]
282. Lagacherie, P.; Bailly, J.S.; Monestiez, P.; Gomez, C. Using Scattered Hyperspectral Imagery Data to Map the Soil Properties of a Region. *Eur. J. Soil Sci.* **2012**, *63*, 110–119. [[CrossRef](#)]
283. Walker, E.; Monestiez, P.; Gomez, C.; Lagacherie, P. Combining Measured Sites, Soilscape Map and Soil Sensing for Mapping Soil Properties of a Region. *Geoderma* **2017**, *300*, 64–73. [[CrossRef](#)]
284. Alkassem, M.; Buis, S.; Coulouma, G.; Jacob, F.; Lagacherie, P.; Prevot, L. Estimating Soil Available Water Capacity within a Mediterranean Vineyard Watershed Using Satellite Imagery and Crop Model Inversion. *Geoderma* **2022**, *425*, 116081. [[CrossRef](#)]

285. Cousin, I.; Buis, S.; Lagacherie, P.; Doussan, C.; Le Bas, C.; Guérif, M. Available Water Capacity from a Multidisciplinary and Multiscale Viewpoint. A Review. *Agron. Sustain. Dev.* **2022**, *42*, 46. [\[CrossRef\]](#)
286. Arrouays, D.; Grundy, M.G.; Hartemink, A.E.; Hempel, J.W.; Heuvelink, G.B.M.; Hong, S.Y.; Lagacherie, P.; Lelyk, G.; McBratney, A.B.; McKenzie, N.J.; et al. GlobalSoilMap: Toward a fine-resolution global grid of soil properties. *Adv. Agron.* **2014**, *125*, 93–134.
287. Sanchez, P.A.; Ahamed, S.; Carre, F.; Hartemink, A.E.; Hempel, J.; Huising, J.; Lagacherie, P.; McBratney, A.B.; McKenzie, N.J.; Mendonca-Santos, M.d.L.; et al. Digital soil map of the world. *Science* **2009**, *325*, 680681. [\[CrossRef\]](#)
288. Saez, J.L.; Corona, C.; Stoffel, M.; Rovéra, G.; Astrade, L.; Berger, F. Mapping of Erosion Rates in Marly Badlands Based on a Coupling of Anatomical Changes in Exposed Roots with Slope Maps Derived from LiDAR Data: Dendrogeomorphic Quantification of Erosion Rates in Marly Badlands. *Earth Surf. Process. Landf.* **2011**, *36*, 1162–1171. [\[CrossRef\]](#)
289. Bretar, F.; Chauve, A.; Bailly, J.-S.; Mallet, C.; Jacome, A. Terrain Surfaces and 3-D Landcover Classification from Small Footprint Full-Waveform Lidar Data: Application to Badlands. *Hydrol. Earth Syst. Sci.* **2009**, *13*, 1531–1544. [\[CrossRef\]](#)
290. Vaysse, K.; Lagacherie, P. Using Quantile Regression Forest to Estimate Uncertainty of Digital Soil Mapping Products. *Geoderma* **2017**, *291*, 55–64. [\[CrossRef\]](#)
291. Zaouche, M.; Bel, L.; Vaudour, E. Geostatistical Mapping of Topsoil Organic Carbon and Uncertainty Assessment in Western Paris Croplands (France). *Geoderma Reg.* **2017**, *10*, 126–137. [\[CrossRef\]](#)
292. Bourennane, H.; King, D.; Chéry, P.; Bruand, A. Improving the Kriging of a Soil Variable Using Slope Gradient as External Drift. *Eur. J. Soil Sci.* **1996**, *47*, 473–483. [\[CrossRef\]](#)
293. Bourennane, H.; King, D. Using Multiple External Drifts to Estimate a Soil Variable. *Geoderma* **2003**, *114*, 1–18. [\[CrossRef\]](#)
294. Martins, B.H.; Suzuki, M.; Yastika, P.E.; Shimizu, N. Ground Surface Deformation Detection in Complex Landslide Area—Bobonaro, Timor-Leste—Using SBAS DInSAR, UAV Photogrammetry, and Field Observations. *Geosciences* **2020**, *10*, 245. [\[CrossRef\]](#)
295. Ghorbanzadeh, O.; Didehban, K.; Rasouli, H.; Kamran, K.; Feizizadeh, B.; Blaschke, T. An Application of Sentinel-1, Sentinel-2, and GNSS Data for Landslide Susceptibility Mapping. *ISPRS Int. J. Geo-Inf.* **2020**, *9*, 561. [\[CrossRef\]](#)
296. te Brake, B.; Hanssen, R.F.; van der Ploeg, M.J.; de Rooij, G.H. Satellite-Based Radar Interferometry to Estimate Large-Scale Soil Water Depletion from Clay Shrinkage: Possibilities and Limitations. *Vadose Zone J.* **2013**, *12*, 1–13. [\[CrossRef\]](#)
297. Deffontaines, B.; Kaveh, F.; Fruneau, B.; Arnaud, A.; Duro, J. Monitoring Swelling Soils in Eastern Paris (France) Through DinSAR and PSI Interferometry: A Synthesis. In *Engineering Geology for Society and Territory—Volume 5*; Lollino, G., Manconi, A., Guzzetti, F., Culshaw, M., Bobrowsky, P., Luino, F., Eds.; Springer International Publishing: Cham, Switzerland, 2015; pp. 195–202. ISBN 978-3-319-09047-4.
298. MacMillan, R.A.; Jones, R.K.; McNabb, D.H. Defining a Hierarchy of Spatial Entities for Environmental Analysis and Modeling Using Digital Elevation Models (DEMs). *Comput. Environ. Urban Syst.* **2004**, *28*, 175–200. [\[CrossRef\]](#)
299. Dobos, E.; Daroussin, J.; Montanarella, L. *An SRTM-Based Procedure to Delineate SOTER Terrain Units on 1:1 and 1:5 Million Scales*; Office for Official Publications of the European Communities: Luxembourg, 2005.
300. Institute for Environment and Sustainability (European Commission. Joint Research Centre). *Developments in Soil Science. In Geomorphometry: Concepts, Software, Applications*, 1st ed.; Hengl, T., Reuter, H.I., Eds.; Elsevier: Amsterdam, The Netherlands, 2009; ISBN 978-0-12-374345-9.
301. Minár, J.; Evans, I.S. Elementary Forms for Land Surface Segmentation: The Theoretical Basis of Terrain Analysis and Geomorphological Mapping. *Geomorphology* **2008**, *95*, 236–259. [\[CrossRef\]](#)
302. Martelet, G.; Truffert, C.; Tourlière, B.; Ledru, P.; Perrin, J. Classifying Airborne Radiometry Data with Agglomerative Hierarchical Clustering: A Tool for Geological Mapping in Context of Rainforest (French Guiana). *Int. J. Appl. Earth Obs. Geoinf.* **2006**, *8*, 208–223. [\[CrossRef\]](#)
303. Coulouma, G.; Caner, L.; Loonstra, E.H.; Lagacherie, P. Analysing the Proximal Gamma Radiometry in Contrasting Mediterranean Landscapes: Towards a Regional Prediction of Clay Content. *Geoderma* **2016**, *266*, 127–135. [\[CrossRef\]](#)
304. Tissoux, H.; Prognon, F.; Martelet, G.; Tourlière, B.; Despriée, J.; Liard, M.; Lacquement, F. Contribution de la spectrométrie gamma aéroportée à la caractérisation et à la cartographie des dépôts silico-clastiques fluviaux dans le val de Loire et en sologne (Centre, France). *Quaternaire* **2017**, *28*, 87–103. [\[CrossRef\]](#)
305. Loiseau, T.; Richer-de-Forges, A.C.; Martelet, G.; Bialkowski, A.; Nehlig, P.; Arrouays, D. Could Airborne Gamma-Spectrometric Data Replace Lithological Maps as Co-Variates for Digital Soil Mapping of Topsoil Particle-Size Distribution? A Case Study in Western France. *Geoderma Reg.* **2020**, *22*, e00295. [\[CrossRef\]](#)
306. Launeau, P.; Girardeau, J.; Sotin, C.; Tubia, J. Comparison between Field Measurements and Airborne Visible and Infrared Mapping Spectrometry (AVIRIS and HyMap) of the Ronda Peridotite Massif (South-West Spain). *Int. J. Remote Sens.* **2004**, *25*, 2773–2792. [\[CrossRef\]](#)
307. Tyler, A.N.; Sanderson, D.C.W.; Scott, E.M. Estimating and Accounting for <sup>137</sup>Cs Source Burial through In-Situ Gamma Spectrometry in Salt Marsh Environments. *J. Environ. Radioact.* **1996**, *33*, 195–212. [\[CrossRef\]](#)
308. Wakefield, R.; Tyler, A.N.; McDonald, P.; Atkin, P.A.; Gleizon, P.; Gilvear, D. Estimating Sediment and Caesium-137 Fluxes in the Ribble Estuary through Time-Series Airborne Remote Sensing. *J. Environ. Radioact.* **2011**, *102*, 252–261. [\[CrossRef\]](#) [\[PubMed\]](#)
309. Bégué, A.; Arvor, D.; Bellon, B.; Betheder, J.; de Abelleira, D.; Ferraz, R.; Lebourgeois, V.; Lelong, C.; Simoes, M.; Veron, S. Remote Sensing and Cropping Practices: A Review. *Remote Sens.* **2018**, *10*, 99. [\[CrossRef\]](#)

310. Bégué, A.; Arvor, D.; Lelong, C.; Vintrou, E.; Simoes, M. Agricultural Systems Studies Using Remote Sensing. In *Remote Sensing Handbook. Vol. II: Land Resources: Monitoring, Modeling, and Mapping*; Thenkabail, P.S., Ed.; CRC Press: Boca Raton, FL, USA; Taylor and Francis Group: London, UK; New York, NY, USA, 2015; pp. 113–130.
311. d’Andrimont, R.; Verhegghen, A.; Lemoine, G.; Kempeneers, P.; Meroni, M.; van der Velde, M. From Parcel to Continental Scale—A First European Crop Type Map Based on Sentinel-1 and LUCAS Copernicus in-Situ Observations. *Remote Sens. Environ.* **2021**, *266*, 112708. [[CrossRef](#)]
312. Ghassemi, B.; Dujakovic, A.; Žóttak, M.; Immitzer, M.; Atzberger, C.; Vuolo, F. Designing a European-Wide Crop Type Mapping Approach Based on Machine Learning Algorithms Using LUCAS Field Survey and Sentinel-2 Data. *Remote Sens.* **2022**, *14*, 541. [[CrossRef](#)]
313. Soussana, J.-F.; Loiseau, P.; Vuichard, N.; Ceschia, E.; Balesdent, J.; Chevallier, T.; Arrouays, D. Carbon Cycling and Sequestration Opportunities in Temperate Grasslands. *Soil Use Manag.* **2006**, *20*, 219–230. [[CrossRef](#)]
314. Bailly, J.S.; Lagacherie, P.; Millier, C.; Puech, C.; Kosuth, P. Agrarian Landscapes Linear Features Detection from LiDAR: Application to Artificial Drainage Networks. *Int. J. Remote Sens.* **2008**, *29*, 3489–3508. [[CrossRef](#)]
315. Bellón, B.; Bégué, A.; Lo Seen, D.; de Almeida, C.; Simões, M. A Remote Sensing Approach for Regional-Scale Mapping of Agricultural Land-Use Systems Based on NDVI Time Series. *Remote Sens.* **2017**, *9*, 600. [[CrossRef](#)]
316. Richer-de-Forges, A.C.; Arrouays, D.; Bardy, M.; Bispo, A.; Lagacherie, P.; Laroche, B.; Lemerrier, B.; Sauter, J.; Voltz, M. Mapping of Soils and Land-Related Environmental Attributes in France: Analysis of End-Users’ Needs. *Sustainability* **2019**, *11*, 2940. [[CrossRef](#)]
317. Arrouays, D.; Mulder, V.L.; Richer-de-Forges, A.C. Soil Mapping, Digital Soil Mapping and Soil Monitoring over Large Areas and the Dimensions of Soil Security—A Review. *Soil Secur.* **2021**, *5*, 100018. [[CrossRef](#)]
318. Minasny, B.; McBratney, A.B. A Conditioned Latin Hypercube Method for Sampling in the Presence of Ancillary Information. *Comput. Geosci.* **2006**, *32*, 1378–1388. [[CrossRef](#)]
319. Roudier, P.; Hewitt, A.; Beaudette, D.E. A Conditioned Latin Hypercube Sampling Algorithm Incorporating Operational Constraints. In *Digital Soil Assessments and Beyond: Proceedings of the 5th Global Workshop on Digital Soil Mapping 2012, Sydney, Australia*; McBratney, A., Ed.; CRC Press: Boca Raton, FL, USA, 2012; ISBN 978-0-415-62155-7.
320. Jourdan, A.; Franco, J. Optimal Latin Hypercube Designs for the Kullback–Leibler Criterion. *ASTA Adv. Stat. Anal.* **2010**, *94*, 341–351. [[CrossRef](#)]
321. Mulder, V.L.; de Bruin, S.; Schaepman, M.E. Representing Major Soil Variability at Regional Scale by Constrained Latin Hypercube Sampling of Remote Sensing Data. *Int. J. Appl. Earth Obs. Geoinf.* **2013**, *21*, 301–310. [[CrossRef](#)]
322. Wadoux, A.M.J.-C.; Brus, D.J.; Heuvelink, G.B.M. Sampling Design Optimization for Soil Mapping with Random Forest. *Geoderma* **2019**, *355*, 113913. [[CrossRef](#)]
323. Orgiazzi, A.; Ballabio, C.; Panagos, P.; Jones, A.; Fernández-Ugalde, O. LUCAS Soil, the Largest Expandable Soil Dataset for Europe: A Review. *Eur. J. Soil Sci.* **2018**, *69*, 140–153. [[CrossRef](#)]
324. Casa, R.; Castaldi, F.; Pascucci, S.; Palombo, A.; Pignatti, S. A Comparison of Sensor Resolution and Calibration Strategies for Soil Texture Estimation from Hyperspectral Remote Sensing. *Geoderma* **2013**, *197–198*, 17–26. [[CrossRef](#)]
325. Gomez, C.; Oltra-Carrio, R.; Bacha, S.; Lagacherie, P.; Briottet, X. Evaluating the Sensitivity of Clay Content Prediction to Atmospheric Effects and Degradation of Image Spatial Resolution Using Hyperspectral VNIR/SWIR Imagery. *Remote Sens. Environ.* **2015**, *164*, 1–15. [[CrossRef](#)]
326. Gholizadeh, A.; Žižala, D.; Saberion, M.; Borůvka, L. Soil Organic Carbon and Texture Retrieving and Mapping Using Proximal, Airborne and Sentinel-2 Spectral Imaging. *Remote Sens. Environ.* **2018**, *218*, 89–103. [[CrossRef](#)]
327. Bitjukova, L.; Scholger, R.; Birke, M. Magnetic Susceptibility as Indicator of Environmental Pollution of Soils in Tallinn. *Phys. Chem. Earth Part Solid Earth Geod.* **1999**, *24*, 829–835. [[CrossRef](#)]
328. Blaha, U.; Appel, E.; Stanjek, H. Determination of Anthropogenic Boundary Depth in Industrially Polluted Soil and Semi-Quantification of Heavy Metal Loads Using Magnetic Susceptibility. *Environ. Pollut.* **2008**, *156*, 278–289. [[CrossRef](#)] [[PubMed](#)]
329. Declercq, Y.; Samson, R.; Castanheiro, A.; Spassov, S.; Tack, F.M.G.; Van De Vijver, E.; De Smedt, P. Evaluating the Potential of Topsoil Magnetic Pollution Mapping across Different Land Use Classes. *Sci. Total Environ.* **2019**, *685*, 345–356. [[CrossRef](#)] [[PubMed](#)]
330. Fialová, H.; Maier, G.; Petrovský, E.; Kapička, A.; Boyko, T.; Scholger, R. Magnetic Properties of Soils from Sites with Different Geological and Environmental Settings. *J. Appl. Geophys.* **2006**, *59*, 273–283. [[CrossRef](#)]
331. Hanesch, M.; Scholger, R. The Influence of Soil Type on the Magnetic Susceptibility Measured throughout Soil Profiles. *Geophys. J. Int.* **2005**, *161*, 50–56. [[CrossRef](#)]
332. Hanesch, M.; Rantitsch, G.; Hemetsberger, S.; Scholger, R. Lithological and Pedological Influences on the Magnetic Susceptibility of Soil: Their Consideration in Magnetic Pollution Mapping. *Sci. Total Environ.* **2007**, *382*, 351–363. [[CrossRef](#)]
333. Ellili-Bargaoui, Y.; Malone, B.P.; Michot, D.; Minasny, B.; Vincent, S.; Walter, C.; Lemerrier, B. Comparing Three Approaches of Spatial Disaggregation of Legacy Soil Maps Based on the Disaggregation and Harmonisation of Soil Map Units Through Resampled Classification Trees (DSMART) Algorithm. *SOIL* **2020**, *6*, 371–388. [[CrossRef](#)]
334. Häring, T.; Dietz, E.; Osenstetter, S.; Koschitzki, T.; Schröder, B. Spatial Disaggregation of Complex Soil Map Units: A Decision-Tree Based Approach in Bavarian Forest Soils. *Geoderma* **2012**, *185–186*, 37–47. [[CrossRef](#)]

335. Odgers, N.P.; Sun, W.; McBratney, A.B.; Minasny, B.; Clifford, D. Disaggregating and Harmonising Soil Map Units through Resampled Classification Trees. *Geoderma* **2014**, *214–215*, 91–100. [[CrossRef](#)]
336. Ellili-Bargaoui, Y.; Walter, C.; Michot, D.; Lemerrier, B. Mapping Soil Properties at Multiple Depths from Disaggregated Legacy Soil Maps in the Brittany Region, France. *Geoderma Reg.* **2020**, *23*, e00342. [[CrossRef](#)]
337. Padarian, J.; Stockmann, U.; Minasny, B.; McBratney, A.B. Monitoring Changes in Global Soil Organic Carbon Stocks from Space. *Remote Sens. Environ.* **2022**, *281*, 113260. [[CrossRef](#)]
338. Viscarra Rossel, R.A.; Hicks, W.S. Soil Organic Carbon and Its Fractions Estimated by Visible-near Infrared Transfer Functions: Vis-NIR Estimates of Organic Carbon and Its Fractions. *Eur. J. Soil Sci.* **2015**, *66*, 438–450. [[CrossRef](#)]
339. Baldock, J.A.; Hawke, B.; Sanderman, J.; Macdonald, L.M. Predicting Contents of Carbon and Its Component Fractions in Australian Soils from Diffuse Reflectance Mid-Infrared Spectra. *Soil Res.* **2013**, *51*, 577. [[CrossRef](#)]
340. Nocita, M.; Stevens, A.; Van Wesemael, B.; Aitkenhead, M.; Bachmann, M.; Barthès, B.; Ben Dor, E.; Brown, D.J.; Clairotte, M.; Csorba, A.; et al. Soil Spectroscopy: An Alternative to Wet Chemistry for Soil Monitoring. In *Advances in Agronomy*; Elsevier: Amsterdam, The Netherlands, 2015; Volume 132, pp. 139–159. ISBN 978-0-12-802135-4.
341. Gallo, B.; Demattè, J.; Rizzo, R.; Safanelli, J.; Mendes, W.; Lepsch, I.; Sato, M.; Romero, D.; Lacerda, M. Multi-Temporal Satellite Images on Topsoil Attribute Quantification and the Relationship with Soil Classes and Geology. *Remote Sens.* **2018**, *10*, 1571. [[CrossRef](#)]
342. Drusch, M.; Del Bello, U.; Carlier, S.; Colin, O.; Fernandez, V.; Gascon, F.; Hoersch, B.; Isola, C.; Laberinti, P.; Martimort, P.; et al. Sentinel-2: ESA's Optical High-Resolution Mission for GMES Operational Services. *Remote Sens. Environ.* **2012**, *120*, 25–36. [[CrossRef](#)]
343. Castaldi, F.; Palombo, A.; Santini, F.; Pascucci, S.; Pignatti, S.; Casa, R. Evaluation of the Potential of the Current and Forthcoming Multispectral and Hyperspectral Imagers to Estimate Soil Texture and Organic Carbon. *Remote Sens. Environ.* **2016**, *179*, 54–65. [[CrossRef](#)]
344. Adeline, K.R.M.; Gomez, C.; Gorretta, N.; Roger, J.-M. Predictive Ability of Soil Properties to Spectral Degradation from Laboratory Vis-NIR Spectroscopy Data. *Geoderma* **2017**, *288*, 143–153. [[CrossRef](#)]
345. Gomez, C.; Adeline, K.; Bacha, S.; Driessen, B.; Gorretta, N.; Lagacherie, P.; Roger, J.M.; Briottet, X. Sensitivity of Clay Content Prediction to Spectral Configuration of VNIR/SWIR Imaging Data, from Multispectral to Hyperspectral Scenarios. *Remote Sens. Environ.* **2018**, *204*, 18–30. [[CrossRef](#)]
346. Ben-Dor, E.; Patkin, K.; Banin, A.; Karnieli, A. Mapping of Several Soil Properties Using DAIS-7915 Hyperspectral Scanner Data—A Case Study over Clayey Soils in Israel. *Int. J. Remote Sens.* **2002**, *23*, 1043–1062. [[CrossRef](#)]
347. Mandal, A.; Majumder, A.; Dhaliwal, S.S.; Toor, A.S.; Mani, P.K.; Naresh, R.K.; Gupta, R.K.; Mitran, T. Impact of Agricultural Management Practices on Soil Carbon Sequestration and Its Monitoring through Simulation Models and Remote Sensing Techniques: A Review. *Crit. Rev. Environ. Sci. Technol.* **2022**, *52*, 1–49. [[CrossRef](#)]
348. Bannari, A.; Pacheco, A.; Staenz, K.; McNairn, H.; Omari, K. Estimating and Mapping Crop Residues Cover on Agricultural Lands Using Hyperspectral and IKONOS Data. *Remote Sens. Environ.* **2006**, *104*, 447–459. [[CrossRef](#)]
349. Defourny, P.; Bontemps, S.; Bellemans, N.; Cara, C.; Dedieu, G.; Guzzonato, E.; Hagolle, O.; Inglada, J.; Nicola, L.; Rabaute, T.; et al. Near Real-Time Agriculture Monitoring at National Scale at Parcel Resolution: Performance Assessment of the Sen2-Agri Automated System in Various Cropping Systems around the World. *Remote Sens. Environ.* **2019**, *221*, 551–568. [[CrossRef](#)]
350. Gomez, C.; Dharumarajan, S.; Lagacherie, P.; Riotte, J.; Ferrant, S.; Sekhar, M.; Ruiz, L. Mapping of Tank Silt Application Using Sentinel-2 Images over the Berambadi Catchment (India). *Geoderma Reg.* **2021**, *25*, e00389. [[CrossRef](#)]
351. Diek, S.; Schaeppman, M.; de Jong, R. Creating Multi-Temporal Composites of Airborne Imaging Spectroscopy Data in Support of Digital Soil Mapping. *Remote Sens.* **2016**, *8*, 906. [[CrossRef](#)]
352. Gasmı, A.; Gomez, C.; Lagacherie, P.; Zouari, H.; Laamrani, A.; Chehbouni, G. Mean Spectral Reflectance from Bare Soil Pixels along a Landsat-TM Time Series to Increase Both the Prediction Accuracy of Soil Clay Content and Mapping Coverage. *Geoderma* **2021**, *388*, 114864. [[CrossRef](#)]
353. Benninga, H.-J.F.; van der Velde, R.; Su, Z. Soil Moisture Content Retrieval over Meadows from Sentinel-1 and Sentinel-2 Data Using Physically Based Scattering Models. *Remote Sens. Environ.* **2022**, *280*, 113191. [[CrossRef](#)]
354. Amazirh, A.; Merlin, O.; Er-Raki, S.; Gao, Q.; Rivalland, V.; Malbeteau, Y.; Khabba, S.; Escorihuela, M. Retrieving Surface Soil Moisture at High Spatio-Temporal Resolution from a Synergy between Sentinel-1 Radar and Landsat Thermal Data: A Study Case over Bare Soil. *Remote Sens. Environ.* **2018**, *211*, 321–337. [[CrossRef](#)]
355. Ojha, N.; Merlin, O.; Molero, B.; Suere, C.; Olivera-Guerra, L.; Hssaine, B.; Amazirh, A.; Al Bitar, A.; Escorihuela, M.; Er-Raki, S. Stepwise Disaggregation of SMAP Soil Moisture at 100 m Resolution Using Landsat-7/8 Data and a Varying Intermediate Resolution. *Remote Sens.* **2019**, *11*, 1863. [[CrossRef](#)]
356. Ojha, N.; Merlin, O.; Suere, C.; Escorihuela, M.J. Extending the Spatio-Temporal Applicability of DISPATCH Soil Moisture Downscaling Algorithm: A Study Case Using SMAP, MODIS and Sentinel-3 Data. *Front. Environ. Sci.* **2021**, *9*, 555216. [[CrossRef](#)]
357. Sabaghy, S.; Walker, J.P.; Renzullo, L.J.; Akbar, R.; Chan, S.; Chaubell, J.; Das, N.; Dunbar, R.S.; Entekhabi, D.; Gevaert, A.; et al. Comprehensive Analysis of Alternative Downscaled Soil Moisture Products. *Remote Sens. Environ.* **2020**, *239*, 111586. [[CrossRef](#)]
358. Loizzo, R.; Guarini, R.; Longo, F.; Scopa, T.; Formaro, R.; Facchinetti, C.; Varacalli, G. Prisma: The Italian Hyperspectral Mission. In Proceedings of the IGARSS 2018—2018 IEEE International Geoscience and Remote Sensing Symposium, Valencia, Spain, 22–27 July 2018; pp. 175–178.

359. Gasmi, A.; Gomez, C.; Chehbouni, A.; Dhiba, D.; El Gharous, M. Using PRISMA Hyperspectral Satellite Imagery and GIS Approaches for Soil Fertility Mapping (FertiMap) in Northern Morocco. *Remote Sens.* **2022**, *14*, 4080. [[CrossRef](#)]
360. Guanter, L.; Kaufmann, H.; Segl, K.; Foerster, S.; Rogass, C.; Chabrilat, S.; Kuester, T.; Hollstein, A.; Rossner, G.; Chlebek, C.; et al. The EnMAP Spaceborne Imaging Spectroscopy Mission for Earth Observation. *Remote Sens.* **2015**, *7*, 8830–8857. [[CrossRef](#)]
361. Matsunaga, T.; Iwasaki, A.; Tsuchida, S.; Iwao, K.; Nakamura, R.; Yamamoto, H.; Kato, S.; Obata, K.; Kashimura, O.; Tanii, J.; et al. Hisui Status Toward FY2019 Launch. In Proceedings of the IGARSS 2018—2018 IEEE International Geoscience and Remote Sensing Symposium, Valencia, Spain, 22–27 July 2018; pp. 160–163.
362. Ben-Dor, E.; Kafri, A.; Varacalli, G. SHALOM: An Italian–Israeli Hyperspectral Orbital Mission—Update. In Proceedings of the International Geoscience and Remote Sensing Symposium, Quebec, QC, Canada, 13–18 July 2014.
363. Lee, C.M.; Cable, M.L.; Hook, S.J.; Green, R.O.; Ustin, S.L.; Mandl, D.J.; Middleton, E.M. An Introduction to the NASA Hyperspectral InfraRed Imager (HyspIRI) Mission and Preparatory Activities. *Remote Sens. Environ.* **2015**, *167*, 6–19. [[CrossRef](#)]
364. Hook, S.J.; Green, R.O. MASTER: HyspIRI Airborne Campaign, Western USA, Summer 2018. 2022. Available online: [https://daac.ornl.gov/MASTER/guides/MASTER\\_HyspIRI\\_Summer\\_2018.html](https://daac.ornl.gov/MASTER/guides/MASTER_HyspIRI_Summer_2018.html) (accessed on 29 May 2023).
365. Gascon, F.; Rast, M.; Celesti, M.; Bogaarts, C.; Nieke, J. Chime: A Copernicus Hyperspectral Imaging Mission for the Environment. *Rev. Française Photogrammétrie Télédétection* **2022**, *224*, 5–8. [[CrossRef](#)]

**Disclaimer/Publisher’s Note:** The statements, opinions and data contained in all publications are solely those of the individual author(s) and contributor(s) and not of MDPI and/or the editor(s). MDPI and/or the editor(s) disclaim responsibility for any injury to people or property resulting from any ideas, methods, instructions or products referred to in the content.